# euro spectra

SCIENTIFIC
AND
TECHNICAL REVIEW
OF THE
EUROPEAN
COMMUNITIES

DECEMBER 1972
VOL. XI
NO. 4

Quarterly
publication

1972 - 4

# Contents

**Five editions:**

English, German, French, Italian and Dutch

**Published and edited by:**

Commission of the European Communities, Directorate-General Dissemination of Information, Rue de la Loi, 200
1040 Brussels. Tel. 350040
or
29, rue Aldringen, Luxembourg
Tel. 29241

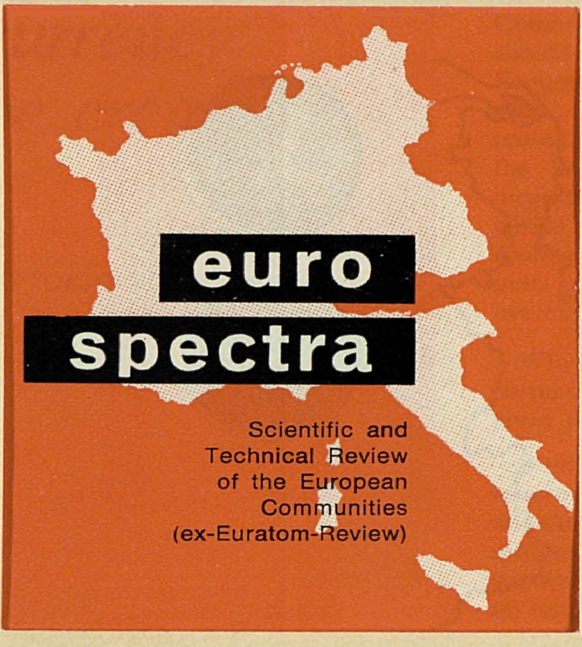

SHOULD YOU WISH TO RECEIVE *euro-spectra* REGULARLY, PLEASE SEND THE ORDER FORM TO:

**Agence et Messageries de la Presse**
Rue de la petite île, 1
1070 Brussels, Belgium
(Postal account 416.69)

*or*

**H.M. Stationery Office**
P.O. Box 569
London S.E. 1 Great Britain

*or*

**European Communities Information Service**
2100 M Street, N.W.
(Suite 707),
Washington, D.C. 20037
U.S.A.

**Yearly subscription rate:**
Europe : 180 Belgian Francs
Other countries:
220 Belgian Francs

**Single copies:**
Europe : 50 Belgian Francs
Other countries:
60 Belgian Francs

# euro spectra

Scientific and
Technical Review
of the European
Communities
(ex-Euratom-Review)

Within a short time during 1972 we lost two personalities who, although from different walks of life, were both staunch and enthusiastic supporters of the European cause — Paul-Henri Spaak and Count Coudenhove-Kalergi.

The summit conference recently held in Paris between the Heads of State of the enlarged Community has yielded practical, if not spectacular, results, especially as regards the Community's monetary problems; it is therefore with gratitude, and not without a certain emotion, that we find the effigies of these European pioneers on the commemorative coins which were recently minted in remembrance of those who have been faithful believers in a united Europe.

**Picture credits:** pp. 93, 102, 104, 105, 109: drawings by Gaston Bogaert, Brussels.

Printed in Belgium by Maison d'Edition s.c
6001 Marcinelle

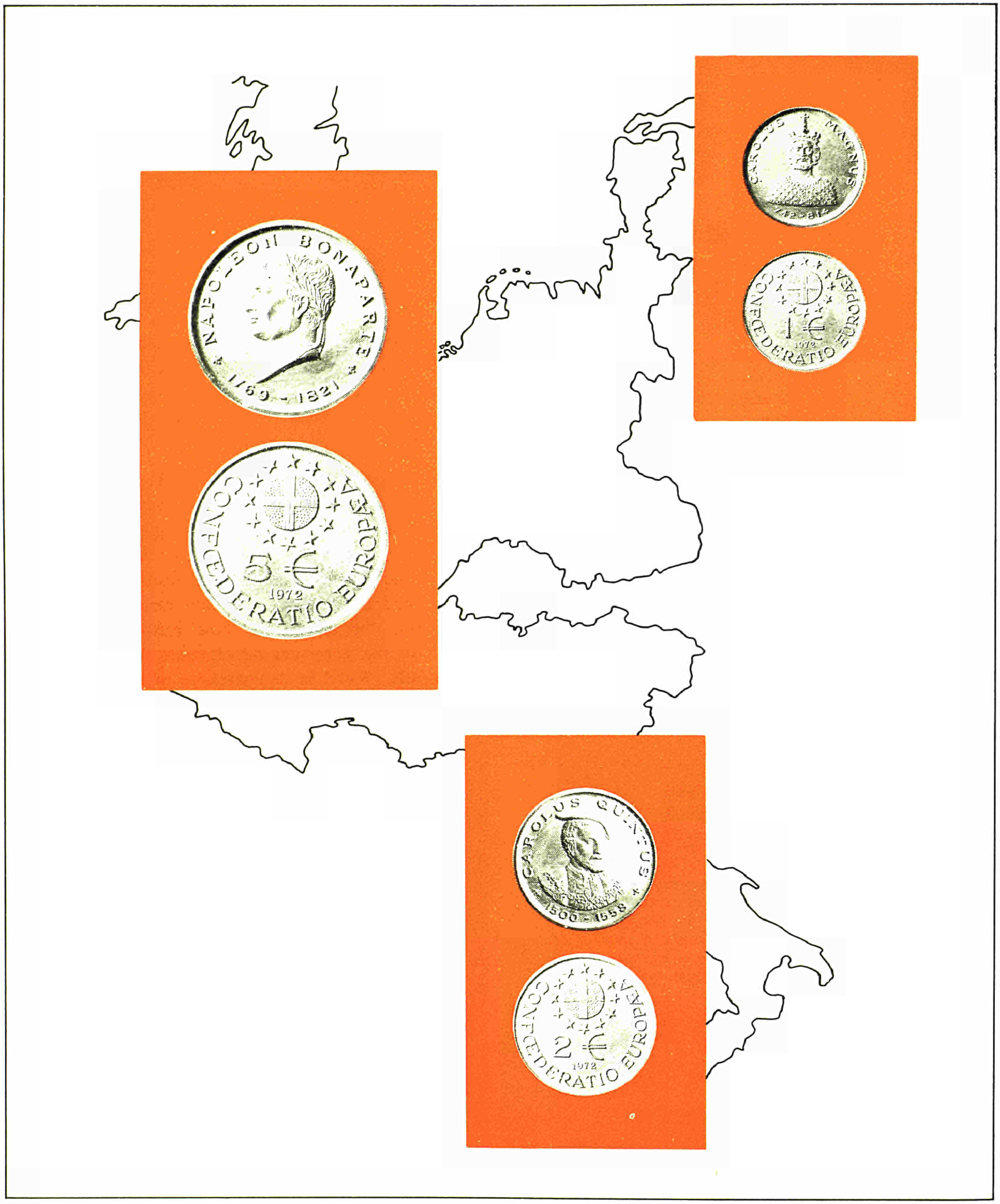
NAPOLEON BONAPARTE
1769 - 1821
CONFEDERATIO EUROPAEA
5 €
1972
CAROLUS MAGNUS
742 - 814
CONFEDERATIO EUROPAEA
1 €
1972
CAROLUS QUINTUS
1500 - 1558
CONFEDERATIO EUROPAEA
2 €
1972

# *Why must a European currency be created?*

VITTORIO PONS

VITTORIO PONS, International Secretary-General of the Paneuropean Union.

ON 9 FEBRUARY 1971, the Commission of the European Communities, following the work of the Werner Committee, laid down the stages which should make way for the achievement of Economic and Monetary Union in ten years. On 15 August 1971 the dollar ceased to be the monetary standard of the Western world; the international monetary crisis which followed—and whose effects still continue to disturb economic relations in Europe—pointed quite clearly to the urgent need for an overall solution.

Why is the creation of a European currency necessary? The answer can be given in two ways.

First of all, the absence of this currency is harmful to Europe; the dollar standard has the continuing effect of reducing the intrinsic value of the national currencies, particularly since the dollar itself is now no longer fixed or covered. The national banks, forced as they are to reckon with the dollar, are coming more and more to resemble branches of the United States Federal Reserve, sometimes even branches of the big American private banks.

The second answer is that the existence of a European currency would immediately solve two problems. The first is that of tourists and travellers, who, for reasons of pure convenience, have adopted the dollar as an "international currency" for their journeys throughout Europe. The second is that of the banks and big companies, which are tending more and more systematically to settle their foreign exchange transactions in Euro-dollars, while the control of these transactions is daily becoming more elusive for any monetary authority, except that of the United States.

The present state of monetary disorder, floating rates of exchange, and the abolition of any form of control, all contribute to general inflation which is tending to become permanent. This situation cannot last for long without having a direct effect on the value of real wages and on the housewife's shopping basket.

How can one create a European currency? History contains a number of instructive precedents. In 1800, before Napoleon's unifying undertaking, the 123 German States issued more than 1 000 coins, and anyone travelling across their territories had to "change" at nearly every staging post. In 1814, there were only 164 coins left in 29 currencies, several of which had the same name, but different values.

The German Reich, founded in 1871 at Versailles, unified all this by adopting, within two years, a single Mark divided into 100 Pfennige for all its territory. All these transformations took place, therefore, in under 75 years and, to take account of national sensibilities, it proved sufficient simply to allow each little State to have the head of its prince or the emblem of its Republic on the reverse side of all coins worth 2 Marks or more, while the Imperial Eagle adorned the obverse.

Since 1792 the United States has also simplified its currency to the extent that six coins are sufficient to cross its territory including Puerto Rico and Guam. And yet there are still 12 monetary districts managed by a Federal Bank.

The twelve governors regulate their exchanges by an Interdistrict Settlement Fund, which is unpublicized and which the user does not even have to know about. Moreover, who notices that these twelve currencies, perfectly convertible between each other, bear a little distinctive sign: B for Boston, C for Chicago, etc...?

Jacques Rueff[1] once said: "Either Europe will be created through currency, or it will not be created at all".

The Chairman of the Banque Lambert, obviously a man of experience, declared recently: "Minting a currency has a huge political significance. In this interim

---

[1] Jacques Léon Rueff is a member of the Académie Française and was President of a Chamber at the Court of Justice of the European Coal and Steel Community from 1952 to 1958, and Judge at the Court of Justice of the European Communities from 1958 to 1962. He is the author of "Le péché monétaire de l'Occident", published in 1971.

period, when Europeans need so much to retain the hope that one day they will be united, acts are called for which are both concrete and spectacular, unifying the symbol and the reality. Few acts could have so great an effect as the creation of a European currency today." He thinks that such a unit of account must make headway, first of all as a banking currency and then finally as common tender. This currency would be issued by the Central Banks in each State and guaranteed by them, either jointly or by a European Reserve Fund. It would therefore have to be governed by "a common monetary authority whose powers would, however, be no wider than those which all the members seem ready to grant it forthwith."

"As soon as the new system is put into practice, its use could become generalized for regulating international exchanges between banks and companies", giving the unit of account "a role equivalent to that which the dollar played before 15 August 1971."

This pragmatic banker describes the near future in the following terms: bank assets in units of account, savings, international loans, (leaving the States "free to decide whether there is a case for retaining a system of exchange controls where it already exists, particularly for capital transactions"), and a free market which would operate perfectly.

He concludes: "Because it will have been in circulation as a means of payments for commercial and financial transactions as a banking currency, the currency will be created in fiduciary form. Tourists in particular would use it for their expenditure. In this way, the psychological conditions for monetary integration would be brought about to the extent that what still remained to be achieved later at the official level would merely seem the natural extension of what was already being practised".

The suggestion of the Chairman of the Banque Lambert seems very realistic. The proof is that the new unit of account would be used by tourists: 100 million people going on seasonal migration across Europe every year. The psychological effect would be considerable. International loans could be issued in units of account, but the need for this is already felt so much that, in January 1971, the European Coal and Steel Community issued a 8% 1970-85 loan for 50 million European Monetary Units, symbolized by the sign "Ɇ", a loan which, moreover, was immediately taken up in its entirety.

How should the new currency be defined? In gold, special drawing rights and gold, or just special drawing rights? Most numerous are the protagonists of an evaluation in terms of gold, and the ambitions of Jacques Rueff are well known. He summarizes them in the following way:

"Doubling the price of gold and generally revaluing reserves of the precious metal are the condition for refunding the dollar balances and the special drawing rights. This revaluation should make it possible to establish a sort of Marshall Plan in reverse by lending to the United States the face-value surpluses acquired by countries which have gold but no balances to be refunded. Practically, all the dollar balances would disappear. The resulting reconstruction of the international monetary system would cause a wave of prosperity and expansion in the West which would be without precedent in history, and would at the same time greatly diminish inflationary pressures".[2]

To return to our unit of account. What should it be called, for the term "unit of account" is not a popular one? French and English experts, and many others, have shown a preference for the English initials *ECU* (*E*uropean *C*urrency *U*nit) which, by a play of words, calls to mind the *écu*, dating from the time of King Louis IX.

The Dutch advertising agency *PRAD* thought of consulting the readers of the American magazine *TIME* in 1971. 1 464 answers were received, from 36 countries, and suggesting 1 200 different names. The name which came up the most often was *EURO*, which obtained 102 votes. Afterwards came the *COMMAR*, mentioned 37 times, the *COMARK* 36 and many other names: Ducat, Talent, Euron, Pax, etc.

The Paneuropean Union questioned the editors-in-chief and directors of European economic and financial newspapers in August 1972, and discovered that they, too, preferred the term *EURO* ("*Handelsblatt*", Düsseldorf, "*La Stampa*", Turin, "*Luxemburger Wort*", for example). Along with extravagant suggestions—a British paper proposed *HOMER*—there was also the proposal of "*The Economist*" of London which is worth noting: *CROWN*, as most of the Community States are monarchies. The same paper opted in second place for *ECU*, which is also favoured by "*The Financial Times*", and "*De Tijd*" of Antwerp. "*The Financial Times*" also proposes *EUROPA*. Whatever it may be called, it is certain that United Europe needs its own unit of account, and the sooner the Ministers of Finance, united in the European Community, decide on its issue, the better it will be.

Pending this decision, the Paneuropean Union has issued a symbolic European currency consisting of nine coins in two series, the aim being to commemorate in this way the 50th anniversary of the first call for unity launched by Count Coudenhove-Kalergi in 1922.

It is hoped that this currency will be more than a symbol: an incentive to spur on the Ministers responsible.

The name has not been chosen: *EURO-ECU-EUROPA-CROWN...*

On the obverse side the great figures of European unification are portrayed. On the reverse are engraved the 12 stars of the Council of Europe flag, surrounding the symbols of European civilization: the sun of Greek wisdom and the cross of Christian inspiration. The whole is rounded off by the inscription *CONFOEDERATIO EUROPAEA* and the symbolic value of each coin expressed in Ɇ.

EUSPA 11-16

---

[2] When these notes appear, the Summit Conference will have taken place and we will know whether Mr Rueff's optimism has influenced the Heads of State or Government meeting in Paris.

# Cavitation

### *Study of microcrack formation and propagation phenomena in creep deformed metals*

GIOVANNI PIATTI, ROBERT LUBEK, ROBERTO MATERA

THE FACT THAT SOME METALS and alloys, e.g., certain types of steel, undergo a loss of ductility at elevated temperatures is a frequent cause of premature failure or breakage in components or structural elements in high-temperature industrial installations [1].

The resultant plastic deformations produced in the majority of cases are time-dependent strain processes known as "creep". Some typical creep curves are shown in Fig. 1. They demonstrate the correlation between operating temperature, operating load and creep rate, so that it is theoretically possible to define the service parameters for a component in such a way that its useful life exceeds the total life of the plant, it being assumed that the component will not fail. In practice, however, the metal may suffer a sudden loss of ductility within certain temperature ranges which may cause premature impairment of the material's properties, resulting in failure of the component. In order to remedy this, knowledge of the processes governing this reduction in ductility and the various factors which delay or speed up these processes is of fundamental importance. However, in certain forms of application (e.g., nuclear installations) the standard problem of ductility loss is complicated even further by the fact that the choice of materials is greatly restricted by the requirements of neutron economy and the materials are stressed in service to the limit of their mechanical strength (e.g., low wall thickness). Also, components which are exposed to intense radiation, such as fuel clads, have an additional tendency to lose ductility on account of the effect of the radiation. Lastly, mention must be made also of the influence of the chemical environment under normal working conditions (oxidation, surface condition, surface microstructure, etc.) which causes intrinsically brittle materials to rupture more easily.

Numerous theoretical and experimental studies have been conducted on the causes and mechanisms involved in this reduction of ductility with reference to steels and other alloys. Broadly speaking, high-temperature embrittlement is characterized by the transition from transcrystalline to intercrystalline fracture. Studies on the formation and propaga-

GIOVANNI PIATTI, ROBERT LUBEK and ROBERTO MATERA are employed in the Materials Division of the Ispra Establishment of the European Communities' *Joint Research Centre.*

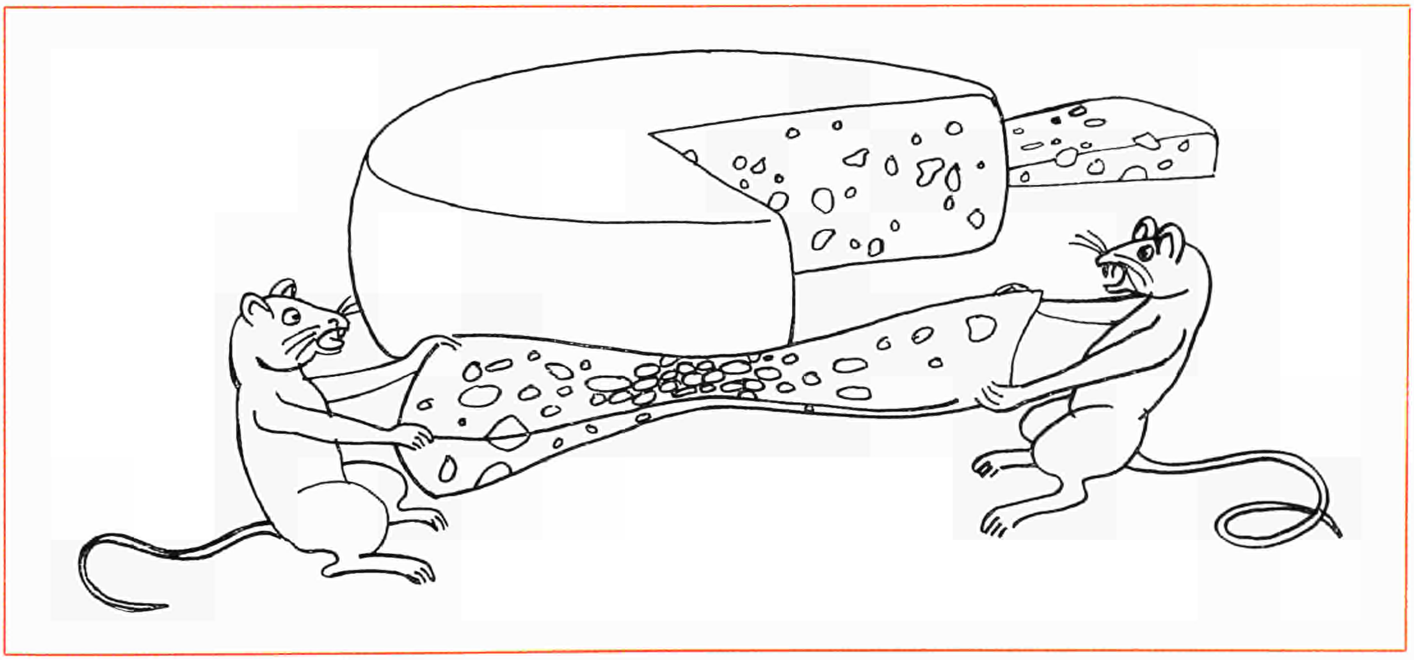

---

[1] The term "elevated temperatures" here is taken to mean those temperatures above 30% or 50% of the absolute melting point, depending on the alloy concerned.

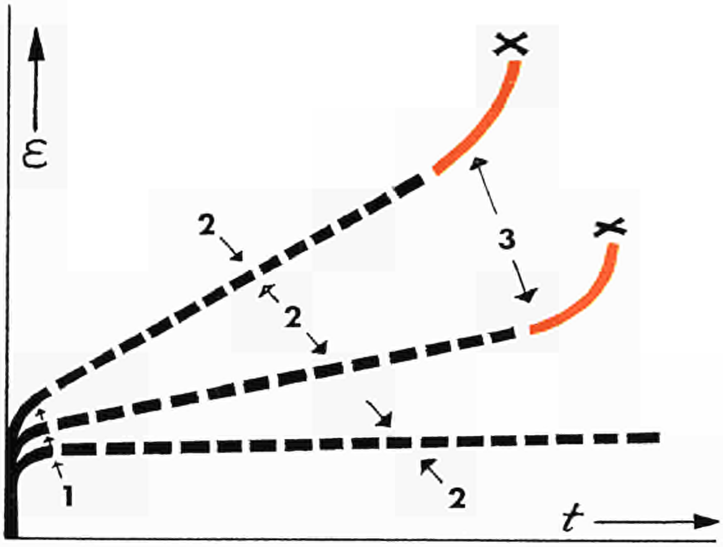

Fig. 1: *Schematic representation of a creep curve in the ε/t diagram. Three different phases can be distinguished: 1) transient creep (solid line) in which the rate of creep decreases from high starting values when the stress is applied; 2) steady-rate creep (broken line), where the creep rate is constant; 3) tertiary creep (in colour), in which the rate of creep increases and rupture always occurs (x = rupture point). Apart from sudden fracture due to ductility loss, the lifetime of a material is determined by its behaviour during steady-state creep.*

tion of microcracks[2] are of fundamental importance among research into the factors which lead to the premature intercrystalline fracture of a material. Investigations have therefore been carried out by numerous workers to examine the entire complex of phenomena involved in the various metals and alloys, from the formation of microcracks and their propagation (i.e., cavitation) to fracture occurring during hot deformation. The results obtained so far are not only of interest from the theoretical standpoint, but can also be applied in practice. Further research is under way in a number of centres, including the Ispra Establishment of the *Joint Research Centre*.

## Working methods

Until about ten years ago, the experimental methods used for studying the formation and propagation of microcracks were limited to metallographic techniques (employing light and electron microscopes). However, it is almost impossible to observe crack propagation accurately under the microscope since the size and shape of the microcavities are altered as a result of the polishing and etching of the ground sections. For some time now the differential density technique has hence been employed instead. This involves carrying out density tests on samples taken from the creep specimens before or after fracture. The real volume of the microcracks formed can then be determined from the relative density changes observed as a function of the parameters governing deformation, namely, strain, time, temperature, load, etc.

It is, of course, impossible to distinguish between the formation and propagation of microcracks using this technique alone. This must be done by determining the number of microcracks per unit volume as a function of the above variables by means of quantitative metallographic analysis employing light or electron microscope techniques. It should also be pointed out that the changes in the shape of the microcracks due to preparation for metallographic analysis are of no major importance as long as

---

[2] The terms "microcrack, microcavity, hair crack and micropore" are taken here to be synonymous.

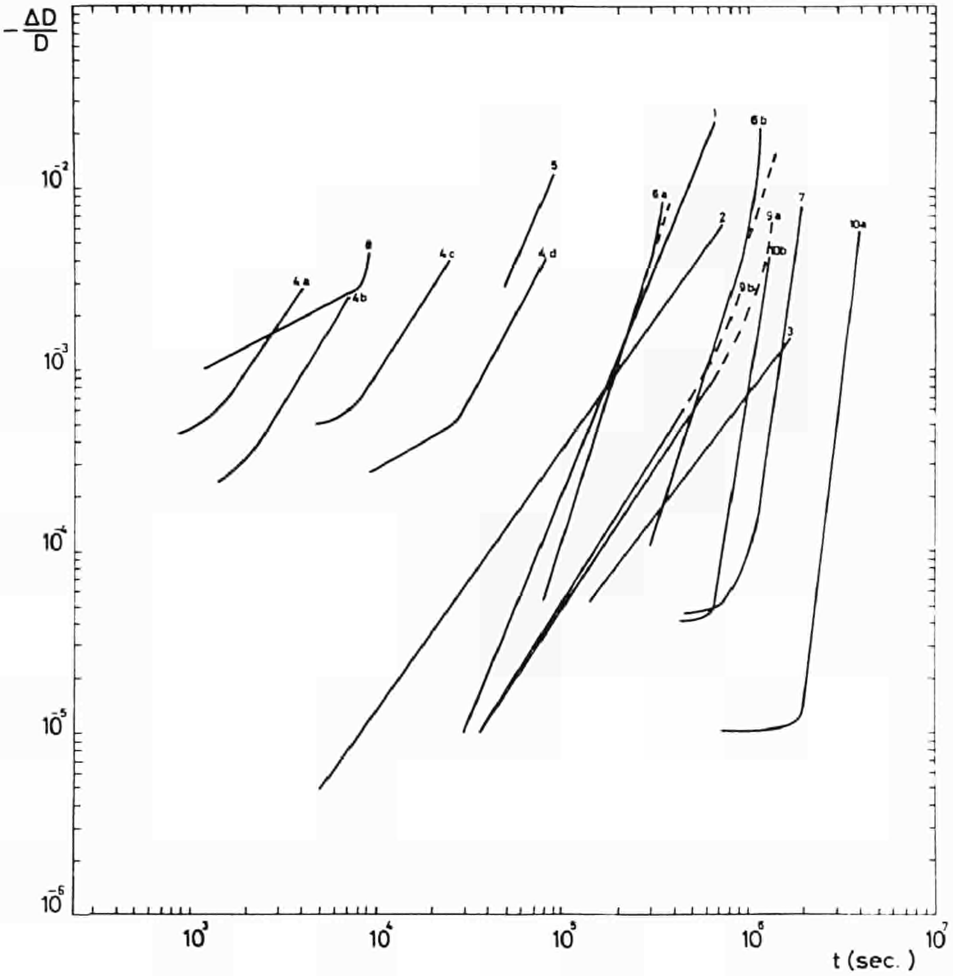

Fig. 2: *The time-dependence of the variation in relative density of various materials creep-deformed under different stress (σ) and temperature conditions. Equation [1] may be applied. In the diagram, the variation (— ΔD/D) in the relative density, which is virtually equal to the porosity, is plotted vs time.*

| | | | |
|---|---|---|---|
| 1 | — Magnesium | σ = 0.5 kg/mm² | T = 300°C |
| 2 | — Copper | σ = 3.64 kg/mm² | T = 400°C |
| 3 | — Copper | σ = 3.5 kg/mm² | T = 400°C |
| 4a | — Nickel 0.1 a/o Pd | σ = 19.1 kg/mm² | T = 503°C |
| 4b | — Nickel 0.1 a/o Pd | σ = 16.1 kg/mm² | T = 503°C |
| 4c | — Nickel 0.1 a/o Pd | σ = 14 kg/mm² | T = 503°C |
| 4d | — Nickel 0.1 a/o Pd | σ = 9.1 kg/mm² | T = 503°C |
| 5 | — Magnox Al 80 | σ = 1.61 kg/mm² | T = 275°C |
| 6a | — Steel 20 Cr/25 Ni irradiated | σ = 4.2 kg/mm² | T = 750°C |
| 6b | — Steel 20 Cr/25 Ni not irradiated | σ = 4.2 kg/mm² | T = 750°C |
| 7 | — Steel 20 Cr/25 Ni/Nb | σ = 9.5 kg/mm² | T = 750°C |
| 8 | — Al—7 % $Al_2O_3$ | σ = 5.9 kg/mm² | T = 450°C |
| 9a | — Steel 1 % Cr/Mo | σ = 19.6 kg/mm² | T = 565°C |
| 9b | — Steel 1 % Cr/Mo | σ = 5.6 kg/mm² | T = 565°C |
| 10a | — Steel AISI 310 | σ = 22 kg/mm² | T = 600°C |
| 10b | — Steel AISI 310 | σ = 25 kg/mm² | T = 600°C |

(σ = specific load)

one is only interested in counting the actual cracks present. Since the following equation is true:

$$(\text{formation}) \times (\text{propagation}) \propto (\text{cavitation})$$

the combination of these two methods (density measurement and quantitative metallographic analysis) enables the parameters governing propagation to be determined accurately.

In addition to this, there are other techniques which can yield useful information on the formation and propagation of microcracks, especially as regards the nature of the fracture. Through analyses made using electron microscopes (transmission microscopy) data can also be obtained on, for example, the interaction between grain boundaries and microcracks and between dislocations and microcracks. Studies such as these can provide valuable information on the physics of solid state which help to improve our understanding of the behaviour of materials.

Scanning electron microscopes are also to be employed in this field on account of their unrivalled capacity for depth of focus, which is particularly useful for detailed analysis of the fracture surfaces of test samples. To obtain data on the type of precipitation and inclusion which are regarded as the origin of cavitation, electron microprobes can be used to perform point analyses of the inclusions and precipitations.

The combined results obtained with all these methods should provide a basis for a phenomenological model of creep cavitation behaviour in a given metal and make it possible to arrive at an equation to describe the parameters governing formation and propagation in order to determine the potential life of a metal. Such models, which represent the relationship between measurable and observ-

Fig. 3: *The time-dependence of the number of microcracks formed per unit volume; the black curve is for copper* [11] *and the coloured curve for Al—Al$_2$O$_3$ (16). Equation* [3] *may be applied. The number of microcracks (n) per cm$^3$ is plotted vs time (sec).*

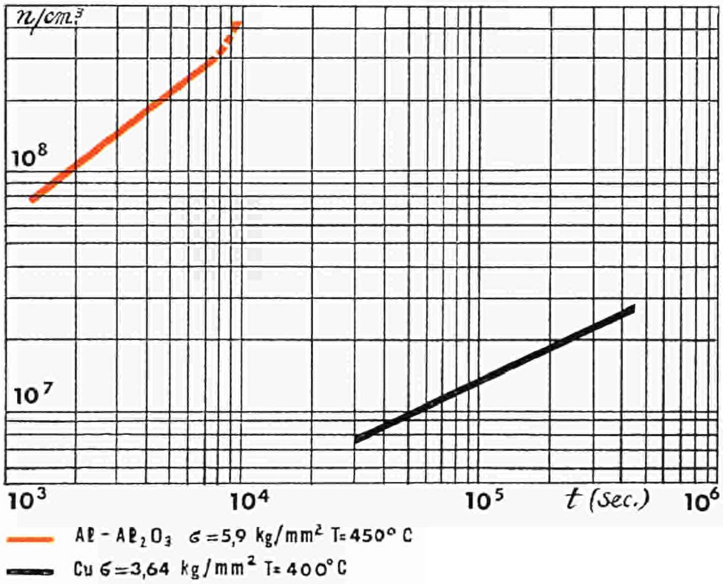

---

Fig. 4: *Schematic representation of the formation of microcavities at grain boundaries: a) formation of a microcavity due to grain boundary sliding near an embedded particle (8); b) formation of a microcavity at a triple point in the grain boundary. Shear stresses act in planes A and C and tensile stresses perpendicular to them in plane B (7). Other models have been suggested to describe these processes, but in all cases it is extremely difficult to obtain sound evidence of their validity.*

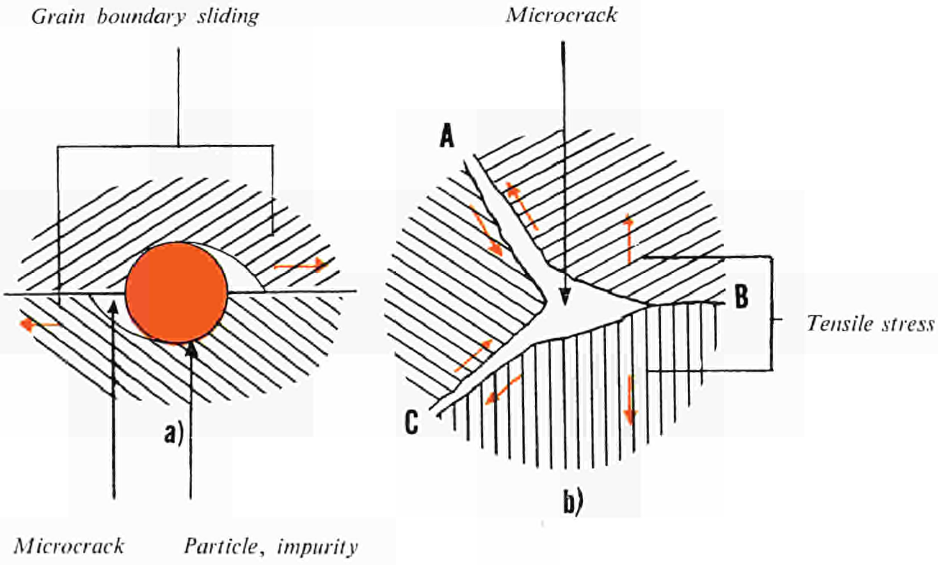

able parameters, are particularly valuable for describing creep processes. Crussard (1) has shown that "an adequate explanation of creep as well as a general view of its formation can be gained by observing the phenomena and building simple models for each individual process involved (steady-state creep, temperature and stress sensitivity, tertiary creep, deformation fracture, *cavitation fracture*, superplasticity, etc.)".

Apart from its theoretical aspect, densimetric analysis also has further practical significance in that combining it with a quantitative metallographic analysis should make it possible to determine with sufficient accuracy the deterioration in the properties of a given metal, the previous history of which as regards mechanical and thermal stress is virtually unknown. The use of such a method of age determination (testing of samples to establish the extent to which the properties of structural materials in thermal installations are impaired) could, in practice, offer considerable economic advantages.

Lastly, it should also be noted that differential density measurement combined with quantitative metallographic analysis can also be employed in the investigation of other problems linked with the brittle fracture behaviour of steels, such as shifts in ductile to brittle transition temperature, radiation-induced changes in tensile strength, etc.

### Cavitation

The cavitation studies conducted hitherto in various laboratories have covered a large number of materials, such as copper, austenitic stainless steels, ferritic steels, magnesium, nickel alloys, aluminium, $Al/Al_2O_3$ composites, zirconium alloys, etc. These studies should be extended to cover a wide range of materials to facilitate evaluation of the results obtained, since it will then be possible to distinguish between the effect of the base metal (Fe, Ni, Al, etc.) and that of structural peculiarities such as dispersed phases, precipitations, carbides, etc.

The relative density changes noted by a number of different authors [(10)...(18)] are shown in the form of a graph in Fig. 2. The measurements are those made on various creep-deformed materials under different test conditions. The variation in the relative density $(V = -\Delta D/D)$, shown as the ordinate in the figure, can

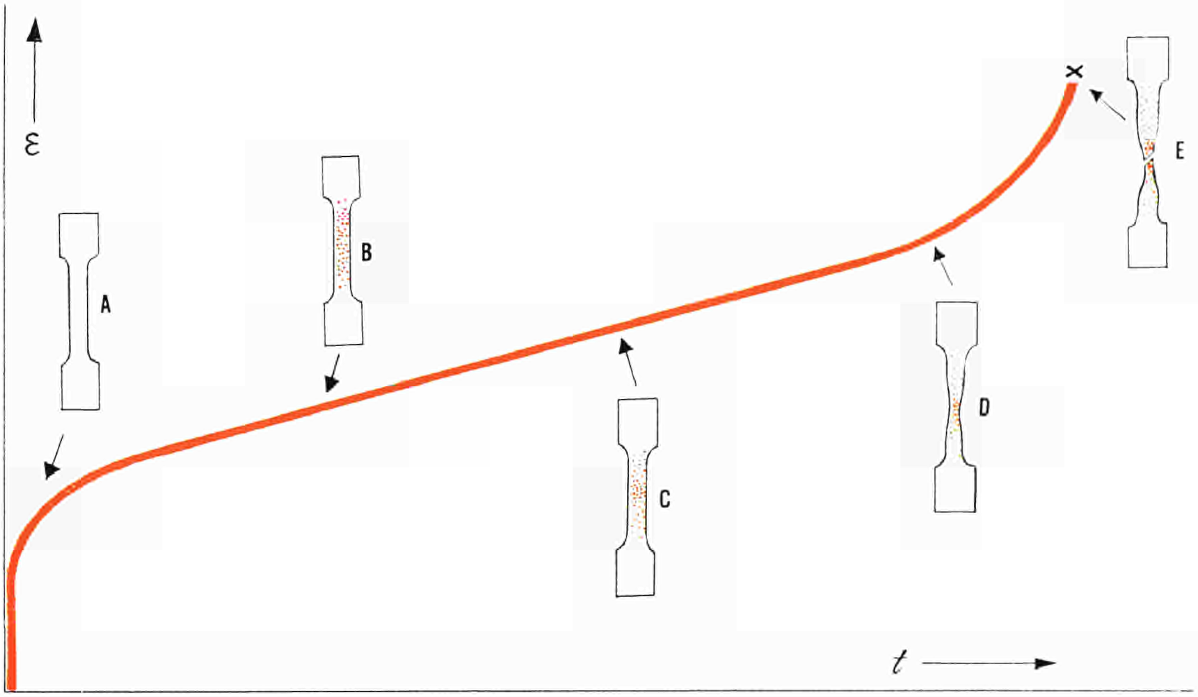

Fig. 5: *Schematic representation of cavitation in a creep sample under specified stress and temperature conditions. The deformation* ε *is plotted as the ordinate and the test time* t *as the abscissa.*

- *A — Strain of the sample with inelastic strain component.*
- *B — Plastic deformation of the sample with probable formation of microcracks. These can hardly be detected using microscope techniques but can be detected by means of density measurements (see Fig. 6).*
- *C — Progressive deformation of the sample. Formation and propagation of the microcracks, chiefly at the grain boundaries. In this phase microcavities are also formed in the grains which can, however, be removed by grain boundary migration.*
- *D — Reduction in area begins. Cavitation is overlapped by the transition from the monoaxial to the triaxial stress condition.*
- *E — Rupture of the sample due to merging of the microcavities and loss of material cohesion at grain boundaries. Figs. 7 and 8 show the fracture areas observed in different materials.*

in practice be taken to equal the porosity[3].

In some cases the time dependence of the change in the relative density V (the cavity volume produced in a metal during a particular cycle, relative to the unit volume) is given by the following equation:

$$V = A \cdot t^{p} \qquad [1]$$

where A is a constant dependent on the load and temperature, and p represents the slope (generally stress-independent) of the curve in the log-log VT diagram.

The exponent p can be regarded as one of the parameters describing the formation and propagation of microcracks. Other parameters can be deduced from the variation of V as a function of other variables such as deformation, temperature, etc.

Some authors have analysed the influence of individual variables on the pore volume V and summarized their findings in the generally valid equation:

$$V = f\,(\sigma,\ \varepsilon,\ t,\ T) \qquad [2]$$

where $\sigma$ is the stress applied, $\varepsilon$ the strain, t the time and T the absolute temperature. For copper (2), the equation is written:

$$V = \text{Const.}\, \varepsilon \cdot t \cdot \sigma^{2.3} \exp\,(-22\,500/RT).$$

Other equations have been written to describe the relationship between the number of microcracks per unit volume (n), the time and other variables. Fig. 3 shows some of the results published in the literature. From the equation

$$n = B \cdot t^{q} \qquad [3]$$

where B is a constant, it is possible to determine the parameter q governing the formation of microcracks. In a combination of these equations, the individual processes of microcrack formation (number of pores per unit volume) and growth ($\nu$) (the volume of one pore) can be separated, the equation

$$\nu = C \cdot t^{p-q}$$

where $\nu$ is the volume of one pore and C is a constant, being used to describe the propagation.

With regard to the formation phenomenon, there seems today to be widespread agreement that microcracks are formed at elevated temperatures by a process of sliding at grain boundaries during which the grain boundary has a kind of entrainment effect on the impurities and precipitations embedded in the structure. Since these particles hinder the slip process, local stress peaks are set up around them which can exert the tensile strength of the material and hence favour the formation of cavities.

The growth phenomena, on the other hand, are not yet fully understood. Whereas on the one hand it is felt that grain-boundary sliding is essential for propagation, another theory considers the diffusion and condensation of lattice vacancies to be the fundamental mech-

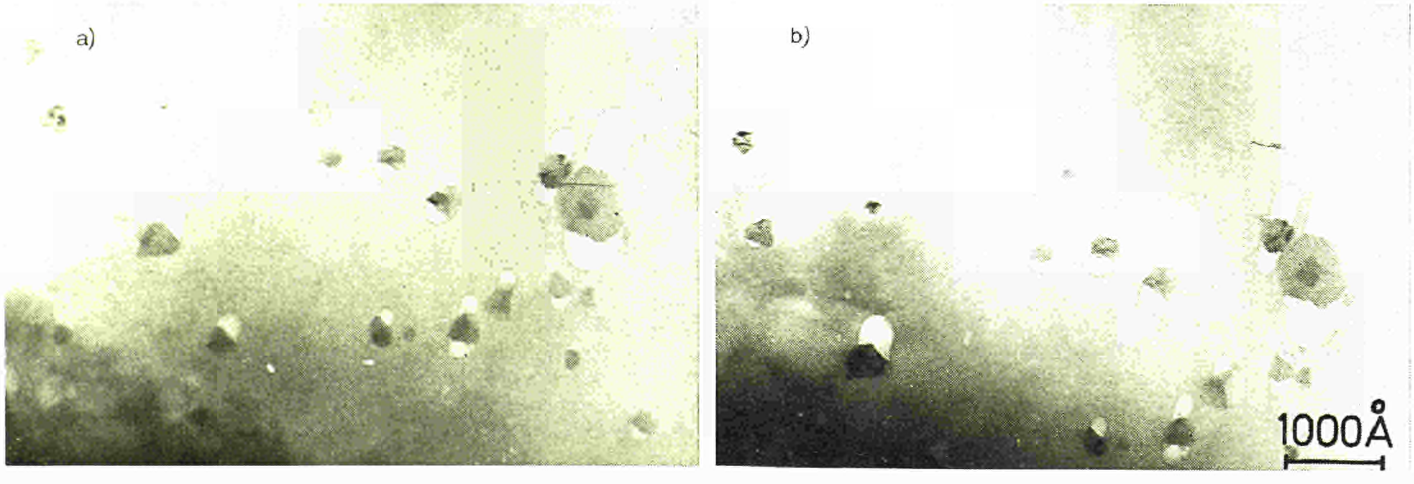

Fig. 6: *Formation of microcavities at the interface matrix (Al)/particles ($\gamma$—$Al_2O_3$) in an Al/$Al_2O_3$ composite material (transmission electron micrograph) (9). Comparison of the two parts of the micrograph a) and b), which represent two successive observations, provides an idea of the growth of microcracks (white) near embedded particles (grey).*

---

[3] The porosity is the coefficient of proportionality relating the total volume of a material to the sum of the individual volumes of all its defects (microcracks, dislocations, vacancies).

anisms involved. The results of recent work in this field suggest, however, that both mechanisms interact in the sense that sliding phenomena are predominant at higher stresses and diffusion at lower stresses. The complex nature of this problem has, however, prevented a complete understanding of these phenomena, and any attempt to obtain detailed information on the processes involved necessitates new and more subtle hypotheses (Fig. 4).

Apart from this first stage in the deterioration of the material's properties, two further stages have been observed, namely, the merging of microcracks and the loss of cohesion in the material at grain boundaries, followed by fracture. A number of theories have also been put forward to explain these processes according to which the ultimate fracture could be caused by a pronounced reduction in the supporting cross-section due to the merging of the microcavities or by a break along the grain boundaries due to the propagation of microcracks by linking.

During tertiary creep, the reduction in area of the test piece governs the transition from the monoaxial to the triaxial state of stress, as a result of which the interpretation of these processes is further complicated. If, however, a relatively rough investigation is felt to be sufficient, it is possible to obtain valid indications as to the nature of these processes. Fig. 5 represents an attempt to show the cavitation process in simplified form as a function of the test time. Figs. 6-8 illustrate the beginnings of cavitation on micrographs of different metals.

The literature [(4), (5), (6)] has published a number of lifetime equations based on the results of differential density measurements. A comparison of the values calculated using these equations with the results obtained from experimental tests indicates that a more detailed differentiation between the formation and propagation processes will enable more sophisticated equations to be formulated. The large number of papers published hitherto on methods of extrapolating the creep rupture behaviour of industrial alloys reveal the importance which is generally attached to these lifetime equations to describe creep phenomena. The outlay in terms of time and money for experiments to establish long-time values is considerably reduced by treating the problem of creep in this way. This is also true if account is also taken of the superimposed effects of radiation in addition to the influence of the temperature (3).

Lastly, tests are being carried out at present at the Ispra Establishment of the *Joint Research Centre* to determine the practical applicability of the age determining technique referred to in this chapter. Density measurements will also be carried out on samples taken from structural components of thermal installations in order to determine the extent of property degradation, the results then being compared with those obtained from laboratory tests on creep samples.

## Measuring methods employed at Ispra

*Determination of the initial properties of materials and creep test conditions* —

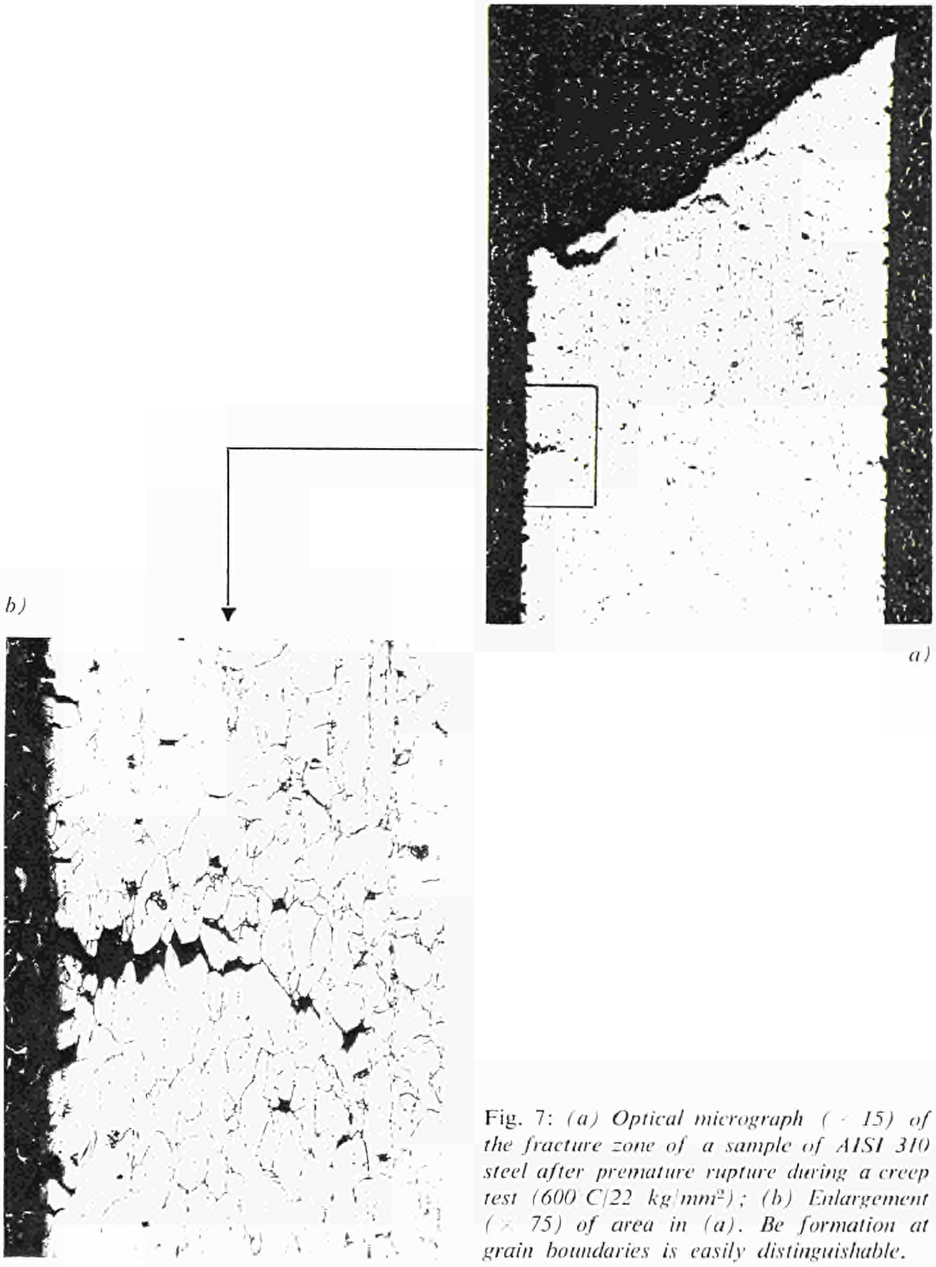

Fig. 7: *(a) Optical micrograph (× 15) of the fracture zone of a sample of AISI 310 steel after premature rupture during a creep test (600 C/22 kg/mm²); (b) Enlargement (× 75) of area in (a). Be formation at grain boundaries is easily distinguishable.*

Determination of the initial properties of a material inevitably covered the composition (chemical analysis), the microstructure (grain size, initial porosity, metallographic analysis of precipitations of oxides, carbide and intermetallic phases) and the evaluation of the degree of homogeneity required for the microscopic measurements planned, and particularly those relating to differential density.

The creep tests are then carried out under given test conditions (stress, temperature, deformation, etc.). During the Zircaloy-2 durability tests, for example, the stress was applied in such a way that fracture occurred after a maximum of 10 000 hours, the temperature being maintained within the range 250-300°C, which is one of particular interest from the point of view of nuclear applications.

These test conditions must be determined individually for each material, due account being taken of the conditions under which it will be used for industrial purposes. Since the aim of these creep tests is to obtain samples for differential density measurements, the tests must as far as possible be carried out under inert atmospheric conditions since (in the present state of the art) the absorption of even minute amounts of oxygen will make it impossible to obtain meaningful results.

*Density measurements* — A differential method had to be developed for precision density measurements. Other authors have devised similar techniques. Owing to the high sensitivity of this method (detection of density changes of less than $10^{-6}$) it is possible to record the changes in density produced by extremely small plastic deformations. Suitable reference samples are required, of course, since the difference in the densities of the actual sample and the reference can only be due to the deformation. All foreign influences, such as annealing, must be carefully eliminated. It may, for instance, be necessary to subject the reference sample to a cycle of heat treatment which corresponds to the temperature cycle maintained when the sample was deformed. In addition to this, further precautions are required to make sure that only the density changes caused by deformation are recorded. Fig. 9 shows a diagram

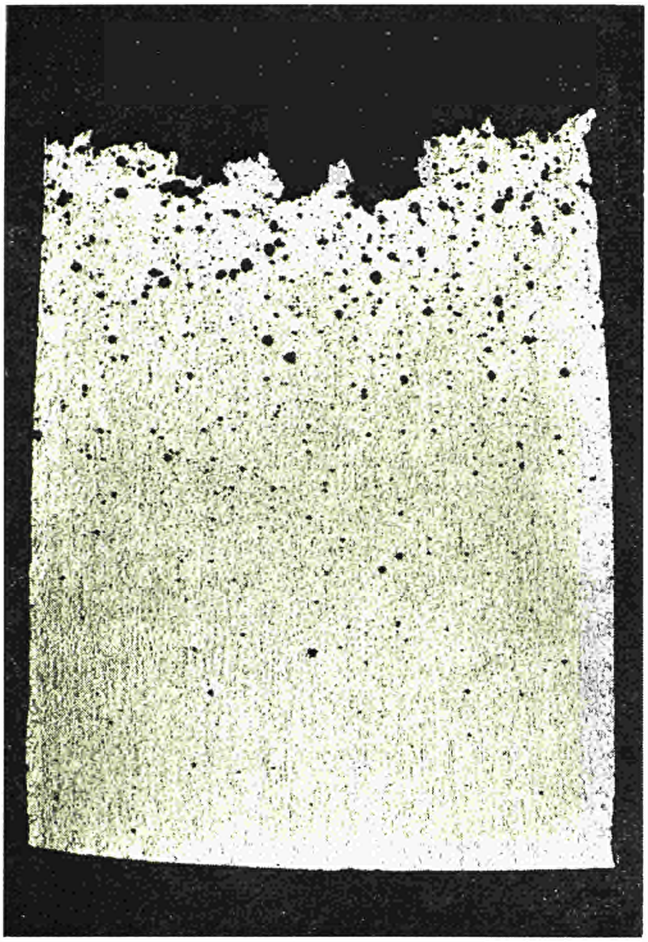

Fig. 8: *Optical micrograph of a creep sample (400°C) of the zirconium alloy Zircaloy-2. Compared with the previous picture, the round shape of the microcavities can clearly be seen. This particular type of microcavity formation is characteristic of creep processes which take place at elevated temperature and under low stress, and brittle fracture can also take place under the same conditions.*

Fig. 9: *Block diagram of the apparatus used in Ispra for differential density measurements.*
*1) Analytical balance (sensitivity 0.01 mg);*
*2) vacuum pump;*
*3) container for buoyancy liquid;*
*4) thermostat;*
*5) weighing box with temperature controlled immersion chamber.*

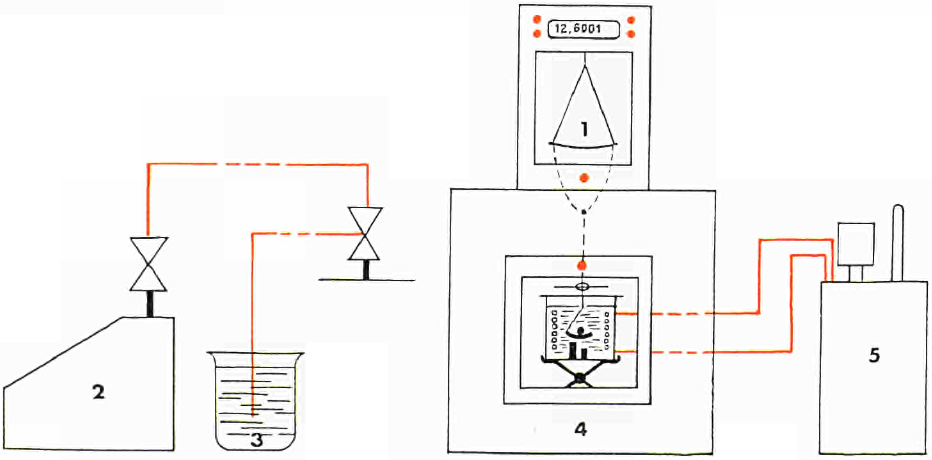

of the apparatus used to measure differential density.

*Quantitative metallographic analysis.* — In any study of microcrack formation and propagation aimed at establishing the number of microcracks formed as a function of the creep conditions (time, stress, etc.), use must be made of quantitative metallographic techniques, as has already been mentioned. Most of the measurements are performed using a TV microscope with which enough samples for a statistical evaluation can be analysed reasonably quickly. By the computer-aided application of equations used in quantitative metallographic analysis, it is possible to determine the spatial distribution and morphology (number, diameter, surface characteristics, form factors) of the microcracks in each individual sample. Fig. 10 shows a block diagram of the apparatus used at Ispra. An automatically controlled program is used to count the microcracks projected onto the screen, so that the metallographer's subjective evaluation is replaced by an objective test value of good reproducibility and all the data contained in the picture can be quantitatively assessed fairly quickly. Without the use of TV microscopes for quantitative analysis, it would be virtually impossible, in practice, to make a simple and significant count of the microcracks present.

EUSPA 11-17

**Bibliography:** (1) C. CRUSSARD: *Mémoires Scientifiques Rev. Métallurg., 66* (1969), p. 333. (2) D.A.WOODFOR: *Metal Sci.J., 3* (1969), p. 50. (3) W. SIEGFRIED, S. ZIMMERING: *Rapport EUR 3752 e* (1968). (4) D. HULL, D.E. RIMMER: *Phil. Mag., 4* (1959), p. 673. (5) M.V. SPEIGHT, J.E. HARRIS: *Metal Sci. J., 1* (1967), p. 83. (6) R.P. SKELTON: *Metal Sci. J., 2* (1968), p.106. (7) C. ZENER: "Elasticity and Anelasticity" University of Chicago Press, Chicago, (1948). (8) J.E. HARRIS: *Trans. AIME, 233* (1965), p. 1509. (9) E. RUEDL: "Proc. European Conference on voids by irradiation of reactor materials" (1971). (10) R.T. RATCLIFFE, C.W. GREENWOOD: *Phil. Mag., 12* (1965), p. 59. (11) A. GITTINS: *Metal Sci. J., 1* (1967), p. 214. (12) R.C. BOETTNER, W.D. ROBERTSON: *Trans. Met. Soc. AIME, 221* (1961), p. 613. (13) P. BOWRING, P.W. DAVIES, B. WILSHIRE: *Metal Sci. J., 2* (1968), p. 168. (14) A. GITTINS: *J. Mater. Sci., 5* (1970), p. 223. (15) A. GITTINS: *J. Mater. Sci., 5* (1970), p. 233. (16) G. PIATTI, H. KELLERER, G. GEEL: *J. Inst. Metals, 99* (1971), p. 283. (17) R.V. DAY: *J. Iron Steel Inst., 203* (1965), p. 279. (18) D. BOERMAN, R. LUBEK, R. MATERA, G. PIATTI: in preparation.

Fig. 10: *Block diagram of the automatic evaluating apparatus used at the Ispra Establishment of the* Joint Research Centre *for quantitative metallographic analysis. A similar layout can be used in conjunction with an electron microscope.*

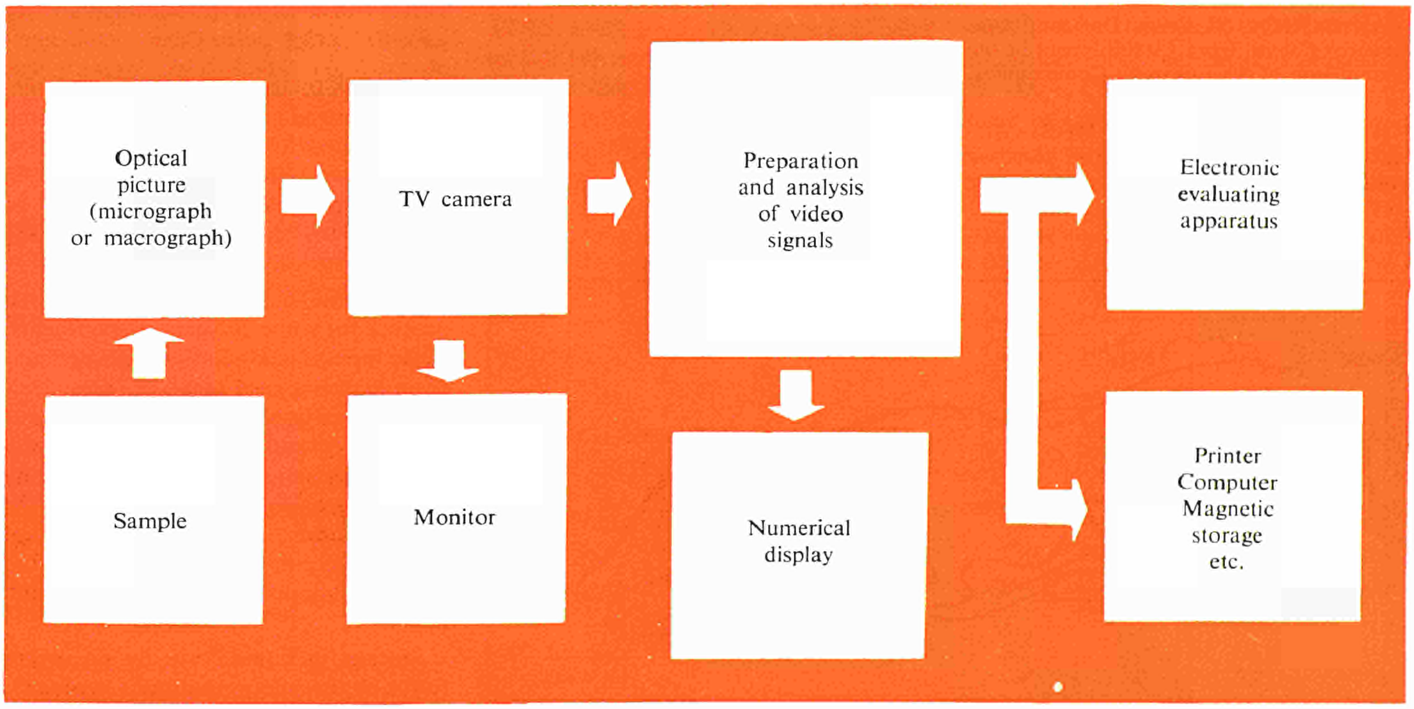

# *Operation "Hot Mole"*

*Self-burial: an elegant solution to the problem of storing high-activity radioactive effluents?*

JEAN DONEA *

### Scale of the radioactive waste storage problem

The storage of radioactive residues from nuclear power plants is a crucial problem, both because of the rapid increase in production levels forecast for the coming years and because of the health and ecological implications of the question, and is one to which a solution must be found in the near future which will afford maximum security in matters of safety and protection.

Table I shows the importance which the problem of the disposal of waste from power reactors is likely to assume in the Community. The data on the production and activity of high-activity waste were taken from an article which appeared recently in this review (1). They are based on the assumption of a minimum nuclear energy development programme in the Six (40 000 MWe installed in 1980, 400 000 MWe in 2000).

On the basis of data supplied in a recent American study (2), we have estimated the thermal power generated by all high-activity products accumulated by the end of every decade.

In this evaluation, it has been assumed that the waste is stored for one year after the irradiated fuel is unloaded and that the reprocessing operations dilute the pure fission products by a factor of 10. The results are shown in the last line of Table I. It will thus be noted that the power generated by the total waste accumulated by the year 2000 will be of the order of 700 MW.

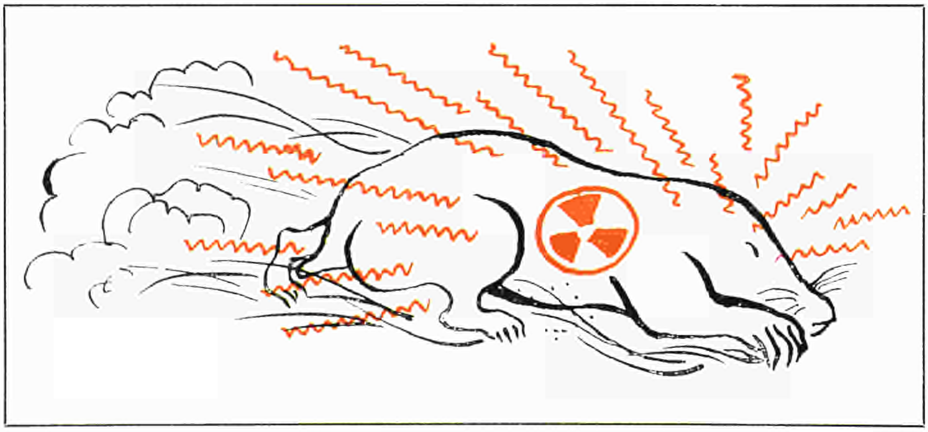

This value, which relates to only a minimum nuclear energy development programme in the Community, represents the power generated by a fair-sized reactor. It is also interesting to ascertain the upper limit to the production and activity of solid waste.

The total energy consumed to date in the Community is of the order of 900 million tce (1 tce = 0.36 MWd). Let us imagine that this energy is at present produced exclusively by nuclear means and that consumption increases by 5% a year. On the assumption that the efficiency of the power plants producing the energy vector (5) is 50% and that 10 000 MWd produce 25 litres of solidified waste (2), by 2000 more than 110 000 m$^3$ of waste will have accumulated, generating something like 15 000 MW.

These figures show clearly that the problem of heat removal from nuclear waste will, in a few decades, be extremely grave. These considerations quite naturally prompt the question as to whether a storage technique is conceivable in which this heat could be used to bury waste in the lower strata of the subsoil. Such a solution is proposed in this article. Before examining it in detail, we propose to review briefly the various storage techniques currently in use.

### Techniques used for storing high-activity waste [(2), (3)]

There is to date no long-term, large-scale industrial practice for the processing of irradiated fuel from power reactors. The disposal of high-activity effluents, in particular, is only just beginning to be a matter of concern to reprocessing plants.

Storage in liquid form has been normal practice for some 20 years; the effluents, in the form of acid solutions, are contained in stainless steel tanks or, if neutralized, in carbon steel tanks. The heat generated by radioactive decay is usually sampled during storage; this is done by immersing coils containing water in the active solution. Around 350 000 m$^3$ of waste are currently stored in the United States in more than 200 underground tanks.

Storage in liquid form by no means fulfils all the safety conditions necessary,

JEAN DONEA, Materials Division, *Joint Research Centre*, Ispra Establishment of the Commission of the European Communities.

* With acknowledgements to Mr S. GIULIANI and Mr L. KESTEMONT for their assistance.

since some 15 carbon steel tanks have so far been known to develop leaks, causing contamination of the soil. Moreover, this type of storage takes up a great deal of space and will not be practicable when the quantities of effluent are much higher than at present.

Laboratories in a number of countries are thus considering the development of other types of radioactive waste storage. To date, storage in solid form seems to be the only technique offering an appreciable reduction in volume and an increase in safety.

Four high-activity liquid effluent solidification processes have been developed and tested in pilot installations during recent years (2). They are: calcination in crucibles, spray solidification, phosphated glass encapsulation and fluidized-bed calcination. Each of these techniques requires a supply of heat to rise the temperature and remove the volatile constituents (water, nitrates). The solid left after cooling is relatively stable chemically.

The American regulations tend to require compulsory solidification of fission products in the five years after fuel unloading and storage in a "graveyard" (salt mine) in the 10 years following discharge. A different philosophy is beginning to emerge which recommends immediate solidification on leaving the reprocessing plant and "cooling" in solid form on site for three to five years.

In these cases, the process used would probably be calcination of effluents with an inert diluent (e.g. aluminium nitrate). The cooled solid could be incorporated in a less leachable medium (such as glass or metal) before being sent to the graveyard.

In Europe no regulations or draft regulations have so far been proposed. It should also be mentioned that studies are currently in progress in the United States to investigate the possibility of dumping the most active waste on other planets or the sun.

## The principle of self-burial

As we have seen, the dissipation of heat in effluents from irradiated fuel reprocessing installations is an important problem in the usual storage techniques.

The self-burial technique which we suggest in this article, on the other hand, consists of using the heat generated by radioactive decay to dump the waste in the deep strata of the subsoil. It is possible to pack high-activity solid waste in suitable containers and bury these in the ground. If the heat generated by the products is higher than a critical value determined subsequently, after a certain period of time the soil in contact with the container will melt and a further burial process, this time automatic, will take place. Provided that the container is denser than the soil and capable of withstanding the melting point of the soil, the self-burial process may be prolonged for as long as the power source, in the form of active waste, can supply the necessary heat.

This, therefore, is a method of burying nuclear waste in the deeper strata of the subsoil, with the threefold advantage of being automatic, elegantly solving the problem of heat dissipation and minimizing the risks of soil contamination.

## Parametric study of self-burial

It is obvious that the use of a self-burial technique, like any other storage method, creates numerous problems. To name only a few, the containers must be made of materials suited to the nature of the subsoil chosen for burial, care needs to be taken in filling and transporting the containers, which are sources of considerable radioactivity and heat, and sites have to be found in places where the subsoil is uniform.

These problems, although important, are not tackled in this preliminary study. The need to investigate them will depend on the answer to the question as to whether self-burial can in fact work using sources in the form of radioactive waste (limited thermal power and decay with time) and containers of feasible dimensions.

Accordingly we shall examine here only the influence of the parameters directly governing the self-burial phenomena, i.e.:

— the external configuration of the containers and their overall dimensions;

Table I: *Estimates of production and activity of radioactive waste in solid form in the Community.*

(a), (b): These figures are based on a minimum nuclear energy development programme (40 000 MWe in 1980, 400 000 in 2000) (1).

(c) : Volumes of waste accumulated at the end of each decade (1).

(d) : To give a tangible idea of the problems posed by storage, we have characterized waste by the heat it generates. The thermal power existing by the end of the decade is due to all the solid waste accumulated at that date. It has been calculated from American data (2) on the assumption that the waste is stored for one year after discharge and that reprocessing causes dilution of the pure fission products by a factor of 10.

| | 1970 | 1980 | 1990 | 2000 |
|---|---|---|---|---|
| (a) Curies discharged per year (× $10^9$) | 0.6 | 6 | 28 | 60 |
| (b) Annual production ($m^3$) | 13 | 130 | 500 | 1 200 |
| (c) Cumulated volumes ($m^3$) | 20 | 650 | 4 000 | 13 000 |
| (d) Estimate of thermal power present (MW) | — | 60 | 250 | 700 |

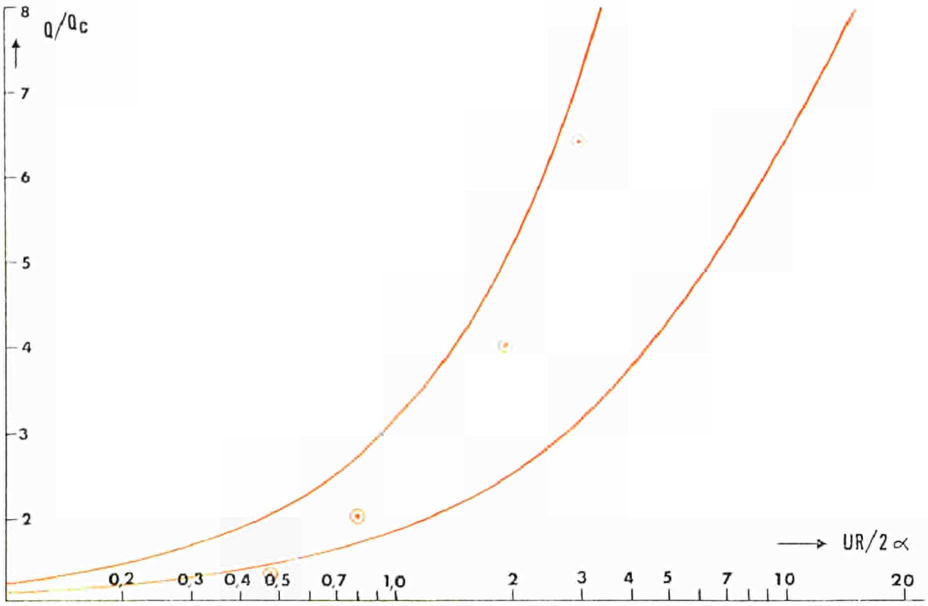

Fig. 1: *Burial rates U attainable with spherical containers are a function of: (a) radius R; (b) ratio between power Q generated by waste and critical power defined by equation [1]; (c) thermal diffusivity $\varkappa$ of soil chosen for burial. At equal available power, the burial rate of a container depends on the mode of distribution of the heat flux over the outer surface of the container. The right-hand curve in the figure is for an isothermal container, and the left-hand curve for uniform distribution of the heat flux over the outer surface of the container.* ○ *Experimental data on the burial of a steel sphere in paraffin.*

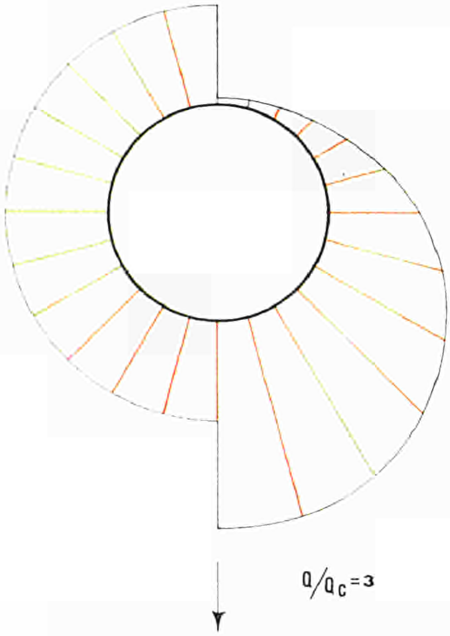

Fig. 2: *Isothermal sphere and uniform flux model. Illustration of the distribution of surface heat flux. The isothermal sphere model has a heat flux concentration in the burial direction and thus, at equal available power, gives a higher burial rate than the model with uniform flux distribution. (The arrow points at the direction of burial).*

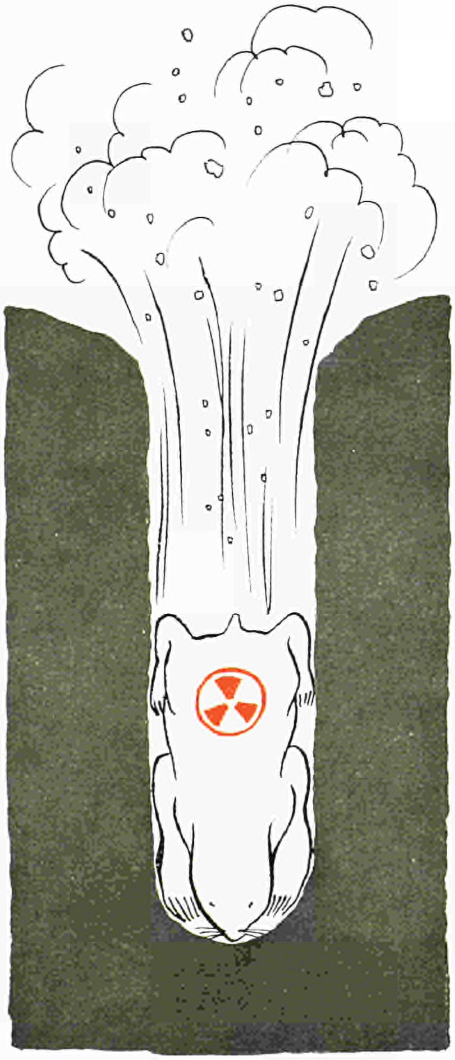

- — the specific power of the heat source and its decay law;
- — the thermal properties of the subsoil.

Any solution to the self-burial problem involves an examination of the movement in the subsoil strata of a heat source of finite dimensions and time-dependent power output.

It will readily be realized that simplifying hypotheses are necessary to make the solution of such a problem feasible.

In order to linearize the differential equations governing the process, it is assumed that the thermal properties of the soil are independent of temperature.

It is also assumed that the temperature field round the container appears stationary to an observer at the heat source. This hypothesis entails a constant rate of burial in an infinite and homogeneous medium. As the power of the source decreases in time, the time must be broken up so that the power of the source can be considered as constant within each interval.

Finally, dipole sources due to melting and freezing of the soil and the effects of viscosity will be disregarded.

In a first analysis, the presence of the container was simulated by applying to the edges of a cylindrical or spherical cavity made in the ground boundary conditions either of uniform thermal flux

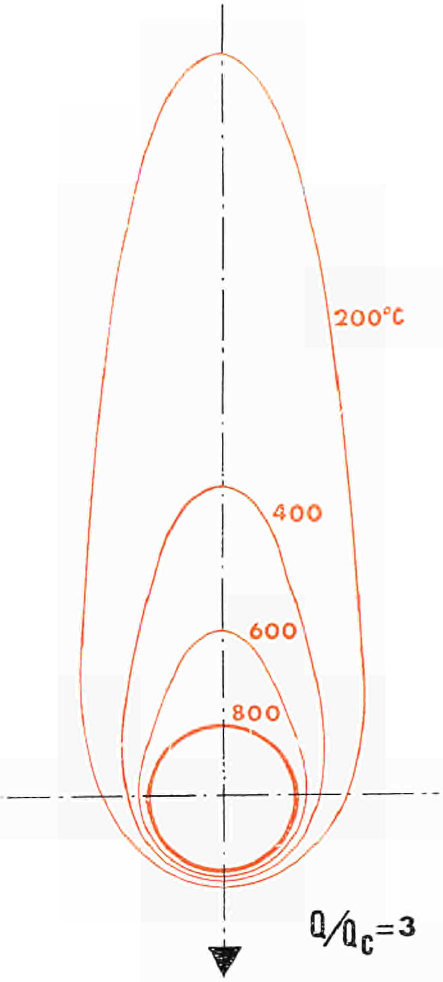

Fig. 3: *Distribution of isotherms round a sphere undergoing burial in salt, on the assumption that the sphere surface is at a uniform temperature equal to the melting point of the salt. (The arrow points at the direction of burial).*

or of uniform temperature equal to the melting point of the soil. This twofold analysis enables the top and bottom limits to the actual behaviour of a container to be defined and should permit a definition of the most interesting areas for a subsequent more detailed study.

**Spherical containers**

*Critical powers* — It can readily be demonstrated (4) that the minimum thermal power $Q_{cr}$ which a spherical container of radius R (cm) must generate to initiate the self-burial process is given by the equation

$$Q_{cr} = 4 \pi R k T_m \text{ (watts)} \qquad [1]$$

where k (W/cm °C) is the thermal conductivity of the soil and $T_m$ (°C) its melting point.

The self-burial of a spherical container holding radioactive waste of power density q (W/cm$^3$) is therefore conceivable only if

$$q > \frac{3 k T_m}{R^2} \qquad [2]$$

To establish an order of magnitude for the power densities involved, let us take the case of burial in salt, for which

$$k \simeq 0.06 \text{ W/cm °C}; \; T_m \simeq 800 \text{ °C}.$$

The minimum power densities are shown in Table II as a function of the container radius.

It is not very easy to determine the values of the power densities available in radioactive waste. These depend very much on the type of fuel, the burnup, the time elapsing between reactor shutdown and storage of the waste and also on the dilution of pure fission products achieved when the fuel is reprocessed.

The power densities can be estimated on the basis of a standard fuel described in an American study (2) and normally chosen as a reference for future reprocessing installations (3).

The reference reactor is a *PWR* burning $UO_2$ enriched with 3.3% $U^{235}$. It operates at a mean power level of 34.8 MW/t and has a burnup of 33 000 MWd/t.

The information in the work cited in the bibliography enables the specific power of the pure fission products to be evaluated as a function of the time elapsing since reactor shutdown. Thus, after 90 days of cooling, the pure products have a power density of 6 W/cm$^3$; after 150 days, the power density drops to 4.4 W/cm$^3$; after one year, it would be 2 W/cm$^3$.

Assuming that reprocessing dilutes the pure products by a factor of 10, radioactive waste of an initial power density equal to several times the final critical densities given in Table II should thus be available.

*Burial rates* — The burial rates obtainable with spherical containers are a function of their dimensions, the power density available and the thermal properties of the soil.

In fact, the problem is a fairly simple one, since all these parameters can be incorporated in two non-dimensional quantities, namely:

— the ratio $Q/Q_{cr}$ of actual thermal power to the critical power defined by equation [1]:

$$Q/Q_{cr} = R^2 \cdot q/3\, k \cdot T_m \qquad [3]$$

— the ratio:

$$Z = \frac{U \cdot R}{2\, \alpha} \qquad [4]$$

of the product of the burial rate and the container radius divided by twice the thermal diffusivity of the soil.

The full investigation of self-burial of spherical containers thus reduces to the construction of a diagram giving the ratio $Q/Q_{cr}$ as a function of the quantity Z.

It is, however, obvious that the value of Z (and therefore the rate) correspond-

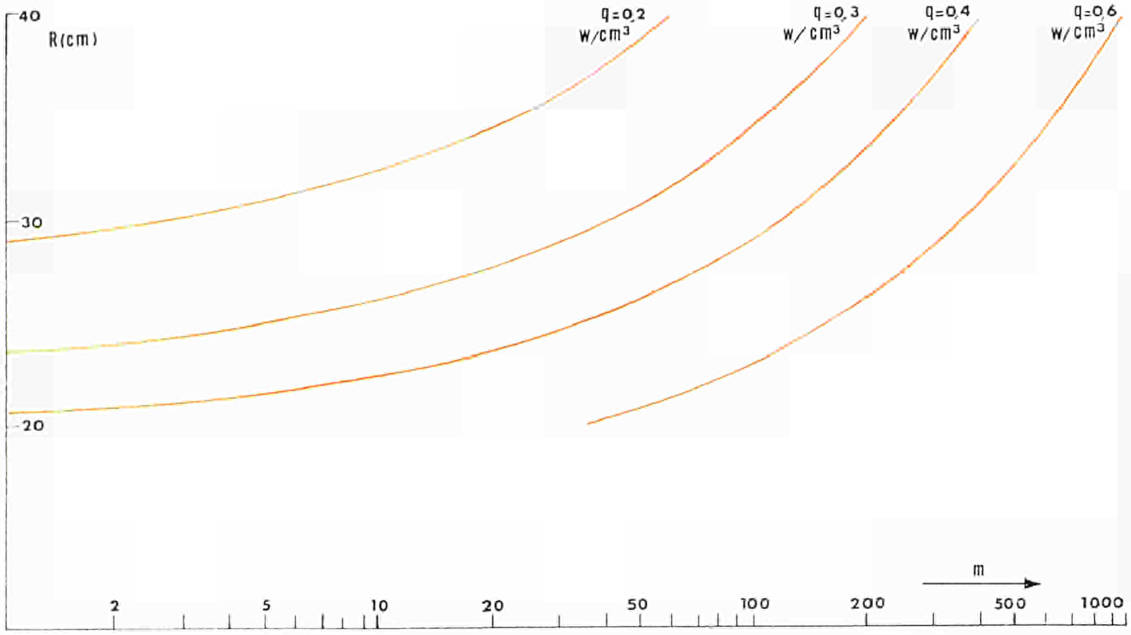

Fig. 4: *The curves show the self-burial depth attainable in salt. They are plotted as a function of the radius R of the spherical container and of the* initial *power density q of the waste. The sphere is assumed to be isothermal; the maximum depth is reached when the power density of the waste is reduced to a value equal to the critical density defined by equation* [2].

ing to a given value of the ratio $Q/Q_{cr}$ depends on the way in which the heat flux is distributed over the surface of the container in contact with the soil. As was previously mentioned, two configurations have been devised in order to describe the actual behaviour of a spherical container.

In the first configuration, it is assumed that the edge of the spherical cavity simulating the container is at a uniform temperature equivalent to the soil melting point $T_m$, whereas at a considerable distance away the temperature remains undisturbed.

The numerical resolution of the temperature field for various values of the ratio Z, followed by integration of heat flux to obtain the power generated by the container, gave the behaviour described by the right-hand curve in Fig. 1.

The second configuration assumes a heat flux uniformly distributed round the edge of the spherical cavity. The results obtained lead to the behaviour law described by the left-hand curve in Fig. 1.

It will be observed that, for equal power, the burial rate of an isothermal sphere is much higher than that of a sphere with uniform flux and the same diameter. The explanation is that, unlike the uniform flux model, the isothermal sphere model has a heat flux concentration in the direction of burial. Fig. 2 shows the heat flux distribution for the two models in question, while Fig. 3 shows the distribution of isotherms round a sphere in motion, it being assumed that the sphere surface is at uniform temperature.

*Burial depths* — The diagrams in Fig. 1, expressed in polynomials, contain all the information required for calculating the burial depths obtainable as a function of container radius and initial power density.

In this calculation, account was taken of the decay in time of the thermal power from the waste, by a process of numerical integration at short time intervals during which the burial rate may be regarded as constant.

The burial depths obtainable were calculated on the assumption that the subsoil consists of salt.

Salt was not chosen at random. Firstly, geologists tell us that there are numerous salt domes in Europe several miles in diameter and more than 1 000 m high (7). Secondly, the melting point of salt is 800 °C, whereas that of other rocks, such as granite, is often over 1 500 °C. It should also be noted that salt domes are integral geological structures, i.e., they contain no faults or other defects. This characteristic is due to the fact that salt is viscous under pressure.

Table II: *Critical power densities as a function of radius of spherical containers. Burial in salt is assumed (melting point 800 °C). Self-burial is possible only if the power density of the waste exceeds the values given. It should be noted that, for containers with a radius of over 30 cm, the critical power densities are very low.*

| R (cm) | 10 | 20 | 30 | 40 | 50 |
|---|---|---|---|---|---|
| $q_{cr}$ (W/cm³) | 1.44 | 0.36 | 0.16 | 0.09 | 0.06 |

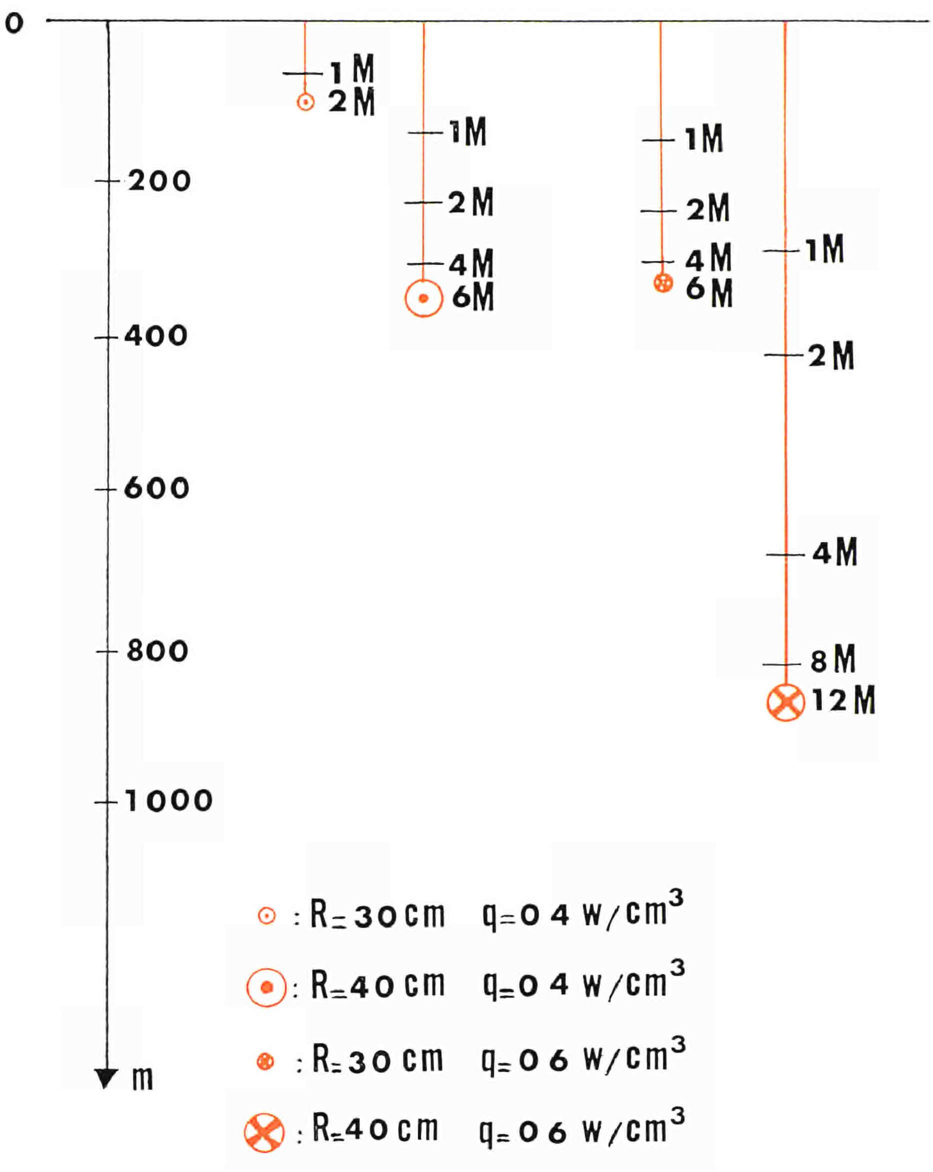

Fig. 5: *The dynamics of the self-burial phenomenon are illustrated by the time curves for the depth reached by four spherical containers of which the radii R and the initial power densities q are given [M month(s)]. The isothermal sphere model is used; burial takes place in salt.*

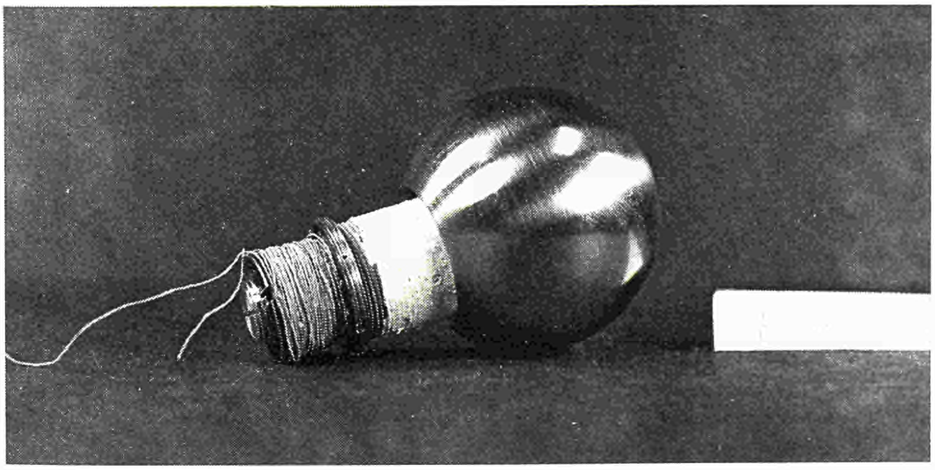

Fig. 6: *A preliminary check on the theoretical results was carried out by burying a steel sphere 5 cm in diameter in a paraffin block. The thermal power was supplied by the Joule effect of a resistor at the centre of the sphere with an external power supply. The results obtained are shown in Fig. 1; they are in fairly good agreement with the estimates of the isoflux model, as might have been expected from the type of experimental device used (low level of internal conduction).*

Fig. 4 shows the self-burial depths obtainable in a salt dome. In order to visualize the dynamics of the phenomenon, Fig. 5 shows the penetration in depth as a function of time. The diagrams refer to isothermal spheres of a radius of 30-40 cm; the initial power density of the waste is 0.4 or 0.6 W/cm$^3$.

*Experimental verification* — In order to check the theoretical data on the burial rates attainable, we carried out an experiment involving the self-burial of a stainless steel sphere 5 cm in diameter in a block of pressed paraffin. The thermal power required is obtained, as Fig. 6 shows, by the Joule effect in an electrical resistor at the centre of the sphere. This resistor is supplied by an external source, the wiring being passed through a zone of liquid paraffin above the sphere.

After an experimental determination of the critical power, we measured the burial rates for various values of the ratio $Q/Q_{cr}$. The experimental points are plotted in Fig. 1; it will be noted that they lie well inside the area delineated by the theoretical curves.

## Cylindrical containers

There are three main phases in the study of the burial of cylindrical containers, as in the case of spherical containers:

- — calculation of critical powers;
- — evaluation of burial rates as a function of power available, geometry and subsoil characteristics;
- — estimation of burial depths attainable.

Only the case of a vertical cylinder has been considered, i.e., with its axis of rotation parallel to the direction of burial.

It is shown (6) that the minimum thermal power which has to be generated by a cylindrical container of radius R (cm) and height/diameter ratio equal to $l$ to start the self-burial process can be found from the equation

$$Q^c_{cr} = 4\,\pi\,R\,k\,T_m \cdot$$

$$\cdot \frac{2\,l}{\log_e\,[2l + \sqrt{1 + 4\,l^2}]} \quad \text{Watts} \qquad [5]$$

Compared with equation [1], this expression shows that the critical power of the cylinder is equal to that of a sphere of equivalent diameter multiplied by a form factor greater than unity and increasing with the value of the height/diameter ratio (see Table III).

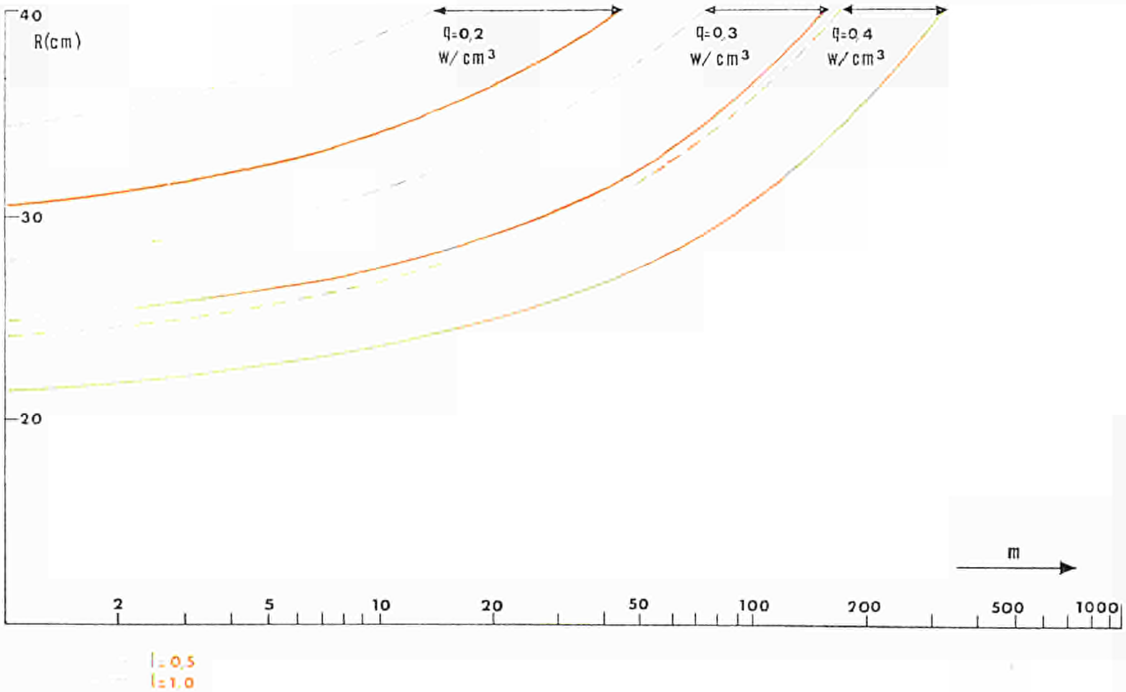

Fig. 7: *Burial depths attainable in salt with cylindrical containers. Two values (0.5 and 1) of the height/diameter ratio were considered. The cylinder surface is assumed to be isothermal; the* initial *power density of the waste is shown.*

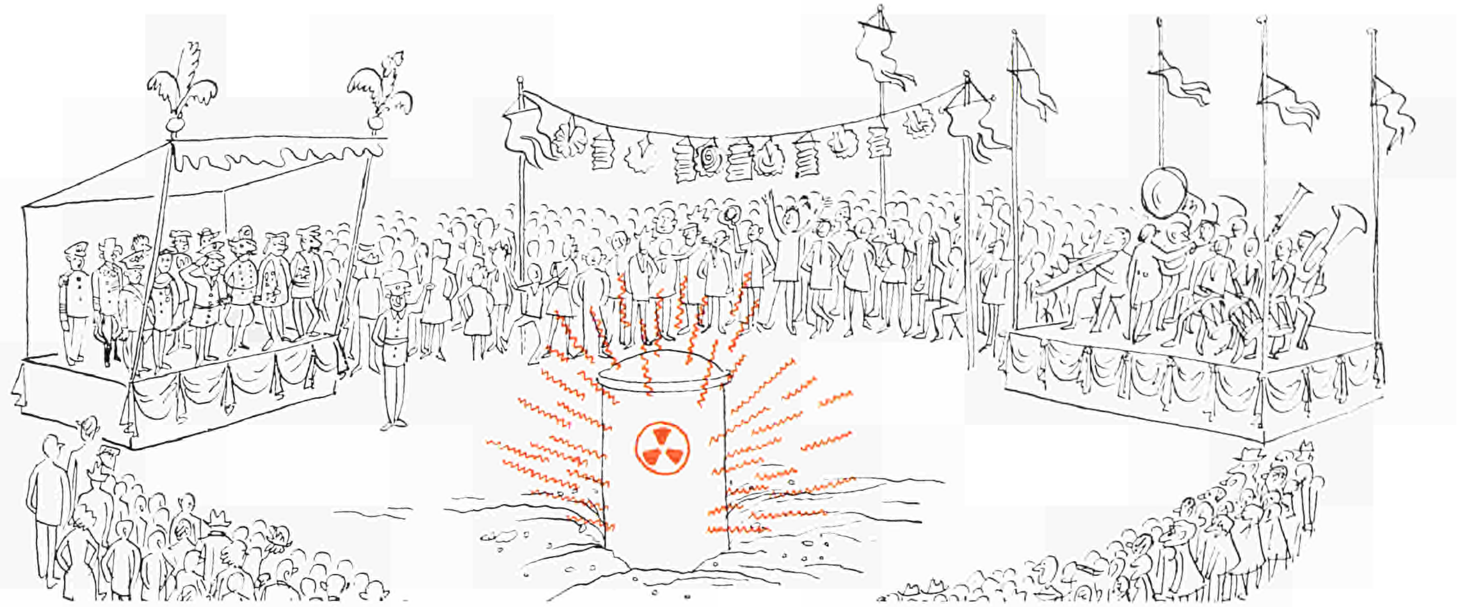

The burial rates are obtained by plotting diagrams giving the ratio $Q/Q^{c}_{cr}$ (actual power/critical power) as a function of the parameter Z defined in equation [4] and the ratio *l*. Only the isothermal model was used in order to approximate the behaviour of a real cylinder.

The burial depths obtainable were calculated for salt and for height/diameter ratios of 0.5 and 1. Fig. 7 shows the depths obtained for the two cylinder types as a function of radius and of the initial power density of the radioactive waste.

**Conclusions**

A preliminary theoretical study, confirmed by laboratory experiments, has shown that the self-burial phenomenon is a fact.

The power densities involved are of an order which allows the use of such a process to be contemplated for the definitive storage of high-activity radioactive waste.

The thorny problem of the removal of the heat generated by radioactive decay is elegantly solved by using this heat as a driving force for the self-burial process tiself. It even becomes desirable for the fission products accumulated in solid form not to be cooled down or diluted too much, so that significant burial depths can be achieved with capsules of acceptable dimensions.

At the same time, it is obvious that we cannot claim, on the basis of the arguments put forward in this article, to have solved all the problems connected with the application of a means of disposing of high-activity waste by self-burial.

What we have tried to do rather is to point out a promising line of research.

EUSPA 11-18

Table III: *Form factor affecting the critical power of a cylindrical container.*

| | Form factor |
|---|---|
| 1 | 1.39 |
| 2 | 1.90 |
| 3 | 2.41 |
| 4 | 2.88 |

**References:** (1) G. GRISON: The creation of a Community system of radioactive waste dumps. *euro-spectra*, 10 (1971) No. 3, pp. 91-94. (2) "Siting of fuel reprocessing plants and waste management facilities", Report compiled and edited by the Staff of the *Oak Ridge National Laboratory*, July 1970. (3) E. DUTILLEUX, Eurochemic, Mol, Belgium, personal information. (We acknowledge with gratitude Mr Dutilleux's interest in our work and the valuable information he has provided.) (4) C.R. EASTON: "Conduction from a finite-size moving heat source applied to radioisotope capsule self-burial", (Douglas Aircraft Company, Santa Monica, California) pp. 209-218 of Thermal Conductivity, Flynn *et al.*, editors, Washington, *National Bureau of Standards*, 1968. (The power for thermoelectric generators on board satellites usually obtained from radioisotope sources. The study in question was undertaken to estimate the consequences of fall-out from a capsule of radioisotopes in the event of an abortive launching). (5) G. de BENI, C. MARCHETTI: Hydrogen, key to the energy market. *euro-spectra*, 9 (1970) No. 2, pp. 46-50. C. MARCHETTI: Hydrogen, master-key to the energy market. *euro-spectra*, 10 (1971) No. 4, pp. 117-129. (These articles show how nuclear energy can cover not only electric power requirements but also most requirements of the energy market). (6) J. DONEA, S. GIULIANI, L. KESTEMONT: Process of self-burial of containers holding high-activity nuclear waste *Report*, *EUR 4903 f* (1972). (7) H. KRAUSE *et al.*: Project for storing radioactive wastes in a salt cavity. Proceedings of the Symposium organized by the *IAEA* and *ENEA* on the Disposal of Radioactive Wastes into the Ground, Vienna, 29 May-2 June 1967. Published by the *International Atomic Energy Agency*.

# *Exoelectron emission dosimetry*

MARTIN OBERHOFER

ONE OF THE METHODS most commonly applied in personnel dosimetry is, it will be recalled[1], film dosimetry, which is based on the blackening of photographic emulsions. In the last few years another technique has been developed —in addition to that using radio-photoluminescence (metaphosphate glasses)— which is based on thermoluminescence and is increasingly employed in present-day dosimetry.

MARTIN OBERHOFER, head of the Personnel Dosimetry Laboratory, Ispra establishment of the *Joint Research Centre* of the Commission of the European Communities.

It was only very recently, i.e. some years ago, that work was commenced on a new dosimetric method, based on the observation that the surfaces of many solid materials emit low-energy electrons during and after various kinds of influences, of either a mechanical or a chemical nature, such as crystallization processes, phase changes, exposure to light or irradiation with particles, X- or gamma-rays. Emission after these influences can be obtained by illuminating the materials with light or by heating them up.

Emission by means of illumination was observed back in 1896 by Elster and Geitel (1), and emission by the application of heat by Klaphecke (2) about 40 years ago.

Many data have been accumulated since then, mostly since 1950. Kramer (3) introduced the term "exoelectron emission", and the abbreviation *EE* used today stems from his early attempt to explain the emission observed as a result of exothermal processes.

Although the phenomenon is now known to be structure-dependent, the term "exoelectron emission" is still used as well as the name "Kramer effect", honouring J. Kramer's outstanding contributions in this field. It was also Kramer who extensively discussed the possible application of exoelectron emission in dosimetry (4) when, in 1957, he noted a linear relationship between exposure to radiation and exoelectron emission (5).

In 1966, then, Kramer succeeded in observing dose-linearity over a dose-range of more than six orders of magnitude by mixing his dosimeter substances with graphite (6), a discovery which resulted in the systematic study of promising materials for their application in exoelectron dosimeters in laboratories here and abroad.

An attempt is made below to explain in some detail the mechanism underlying exoelectron emission on the basis of the band model (7) and to give an idea of the measuring techniques used now, following this with a brief survey of the present state of the art.

## Mechanism of exoelectron emission

By analogy with luminescence, a process which is observed parallel to exoelectron emission [(8), (9)], it is at present assumed that the emission of electrons from the surfaces of solids is connected with the energy deposition in the crystallites of the materials in question by electron transitions between lattice imperfections. The energy deposition, which will subsequently be referred to here as the "excitation process", causes electrons to move the valence band to

---

[1] See K. Becker: "Film dosimetry: a thing of the past?" *euro-spectra*, Vol. VI (1967), No. 3, pp. 78-83.

the conduction band, as is shown in Fig. 1.

The energetic position of the traps (the "trap depth") is characteristic of the material used. There may be different kinds of trap with various trap depths. The higher the deposited energy (e.g. the absorbed radiation dose), the more traps will be filled up with electrons from the valence band.

After the excitation process the electrons can be liberated from their traps by putting more energy into the solid, either optically in the form of light, or thermally in the form of heat. This process is called "stimulation", the term optical and/or thermal stimulation being used. This process is indicated by number 4 in Fig. 1. In both kinds of stimulation electrical conductivity, luminescence and exoelectron emission are noted.

Luminescence (thermoluminescence—*TL*—if the stimulation is thermal) occurs if the electrons return from the conduction band to their ground state, passing through so-called "acceptors". This is shown by the vertical line numbered 5.

Optically stimulated exoelectron emission (usually abbreviated to *OSEE*) and thermally stimulated exoelectron emission (*TSEE*) occur when electrons leave the surface of the material either via the conduction band, if they were trapped in volume traps, or without passing through the conduction band in the case of the surface traps. The energy necessary for this process is given by the trap depth and the work function.

The intensity of the exoelectron emission is related to the number of trapped electrons and thus to the excitation energy or dose. Proportionality is expected as long as the available traps are not exhausted. With increasing filling up of the traps saturation takes place (saturation effect).

A low trap depth may cause "fading" at room temperature, as the thermal energy present is then sufficient to empty the traps with time. The fading characteristics of a material improve for increasing trap depth. The mean energy of the exoelectrons is about 1 eV (10). It was estimated that the exoelectrons originate within a surface layer of a thickness of the order of the mean free path of thermal electrons [(11), (12)]. More recent studies indicate that the detectable exoelectrons originate in a material layer not thicker than 100 Å (13).

## Detection of exoelectrons

In early work exoelectrons were mainly counted with point counters, Geiger-Müller counters and multipliers later being used also. In some special cases the electron emission was measured with electrometer systems. Owing to their low energy the exoelectrons must pass directly into the detector. Thus, in the case of a Geiger counter, the counter must be of the open type. Fig. 2 shows such a counter, which is at present employed together with high-resolution proportional counters in various laboratories for dosimetric studies. Details of the sample-detector arrangement shown in Fig. 2 can be seen in Fig. 3. Fig. 4 gives the block diagram of the accessory instrumentation for the counter.

The result is a curve with one or more emission maxima at characteristic temperatures corresponding to traps of different trap depths. As in thermoluminescence work, this curve is called the "glow curve", or more specifically the "*TSEE* curve", sometimes also the "trap spectrum". Figs. 5 and 6 show such curves obtained with gamma-

Fig. 1: *Fairly simplified schematic band model for explaining luminescence and exoelectron emission from solids.*
*By way of radiation absorption electrons are lifted from the valence band into the conduction band (number 1). After having stayed there for a while (number 2), they drop into the so-called "traps" (number 3) which may be located within the solid (volume traps) or at its surface (surface traps). The energetic position of the traps — "trap depth" — is characteristic of the material used. By putting more energy into the solid (stimulation) the electrons can be liberated from the traps by lifting them first up into the conduction band (number 4). If from there they return then under emission of light (hν) into their original place passing the so-called "acceptors" (number 5), one talks of luminescence [thermoluminescence* (TL) *if the stimulation is thermal]. Exoelectron emission occurs if the electrons leave the surface of the solid (number 6). This case requires an energy supply not less than the sum of the trap depth and the work function. In the case of thermal stimulation, one talks of "thermally stimulated exoelectron emission" (abbreviated:* TSEE*); in the case of optical stimulation, of "optically stimulated exoelectron emission" or, abbreviated,* OSEE.

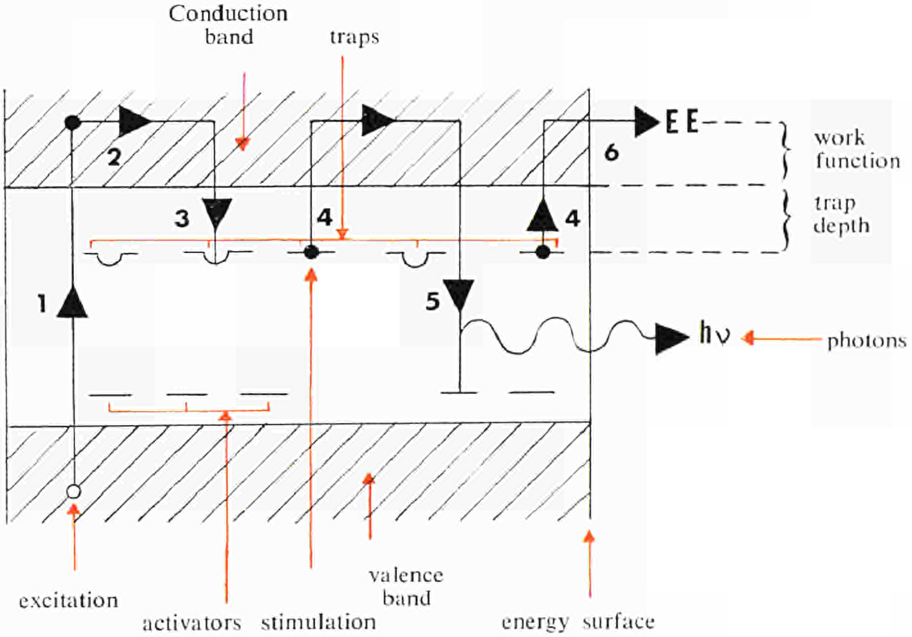

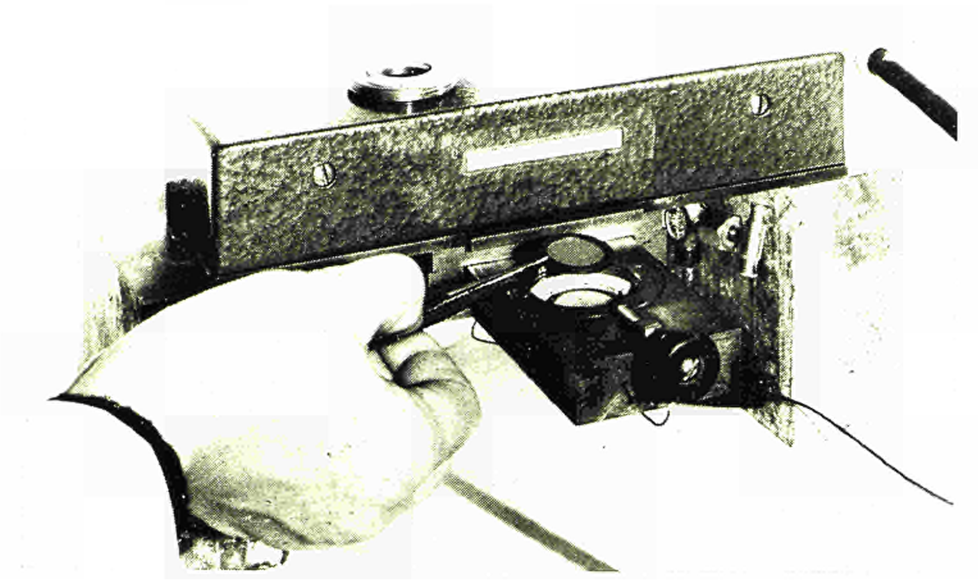

Fig. 2: *Overall view of a high-temperature* TSEE *Counter used at Oak Ridge National Laboratory* (ORNL) (24).

irradiated beryllium oxide and with lithium fluoride powder, both mixed with graphite, the heating-rate being 1°C/sec. For integral dosimetric purposes either the peak height is measured or—and this gives better results—the area under the peak by taking an integral count within

Fig. 3: *Cross-section of the* ORNL *counter shown in Fig.2. The counter, a gas-flow counter, was designed for thermal stimulation, which presents less several problems than optical stimulation. The sample, which is inserted into a slide, is heated with a small plate underneath it. In order to avoid heating up the counter and thus impairing its counting characteristics (plateau shrinkage), the lower part of it is cooled with water. In a later version of the same type of counter the whole sample-slide was cooled.*

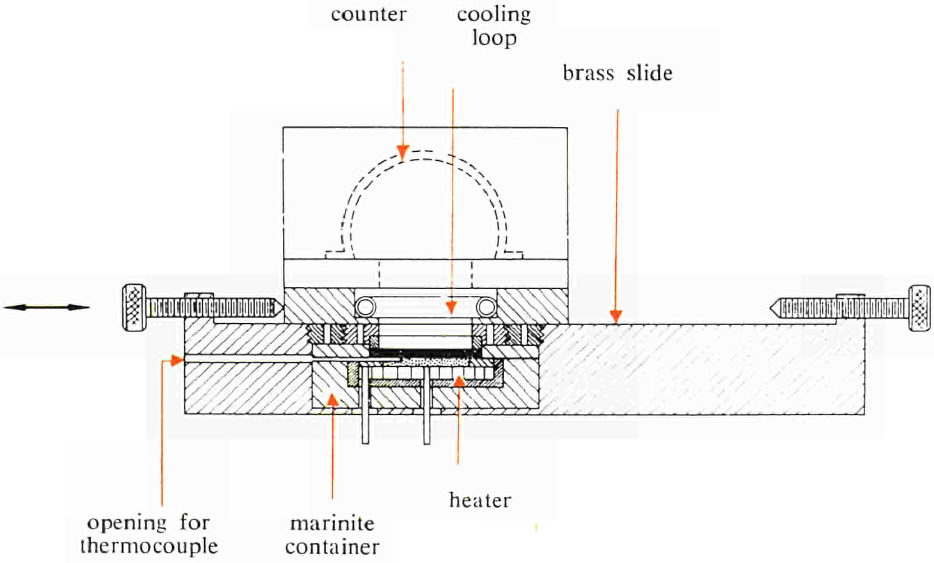

a suitable temperature interval, e.g. 150-350°C in the case of BeO.

## Dosimetric properties of promising EE materials

Many substances, mostly ionic crystals, have been investigated as potential exo-electron dosimeters [(4), (14), (15), (16)]. In the course of these studies it was found that some substances are extremely sensitive to radiation. Kramer (15) had previously reported that doses as low as a few μR can be detected with $CaSO_4$ and that it might be possible to detect a tenth of a μR. This is the main reason why exoelectron dosimetry is attracting so much interest at present.

Exoelectron dosimetry offers other striking advantages, such as the wide dose range obtainable by "diluting" the *EE* materials with non-exoelectron-emitting electrically conductive substances, e.g. graphite, and by making use of electrometer-type readers in addition to counting devices.

By means of optical stimulation Kramer (18) even obtained linearity over eight orders of magnitude with $SrSO_4$ mixed with graphite, as can be seen in Fig. 7.

With *EE* it might be possible to measure doses even as high as $10^8$ R.

Another feature of *TSEE* is the *LET*[2] dependence of the *EE* for some substances, which makes it possible to differentiate between various kinds of radiations. Typical examples are the alkaline earth sulphates $CaSO_4$, $SrSO_4$ and $BaSO_4$.

Fig. 8 shows the *TSEE* curves for $CaSO_4$ exposed to alpha and gamma radiation. The peak/height ratio can be used for determining the effective linear energy transfer (*LET*) (19). Neutron dosimetry in mixed radiation fields might be possible in this way if a proton

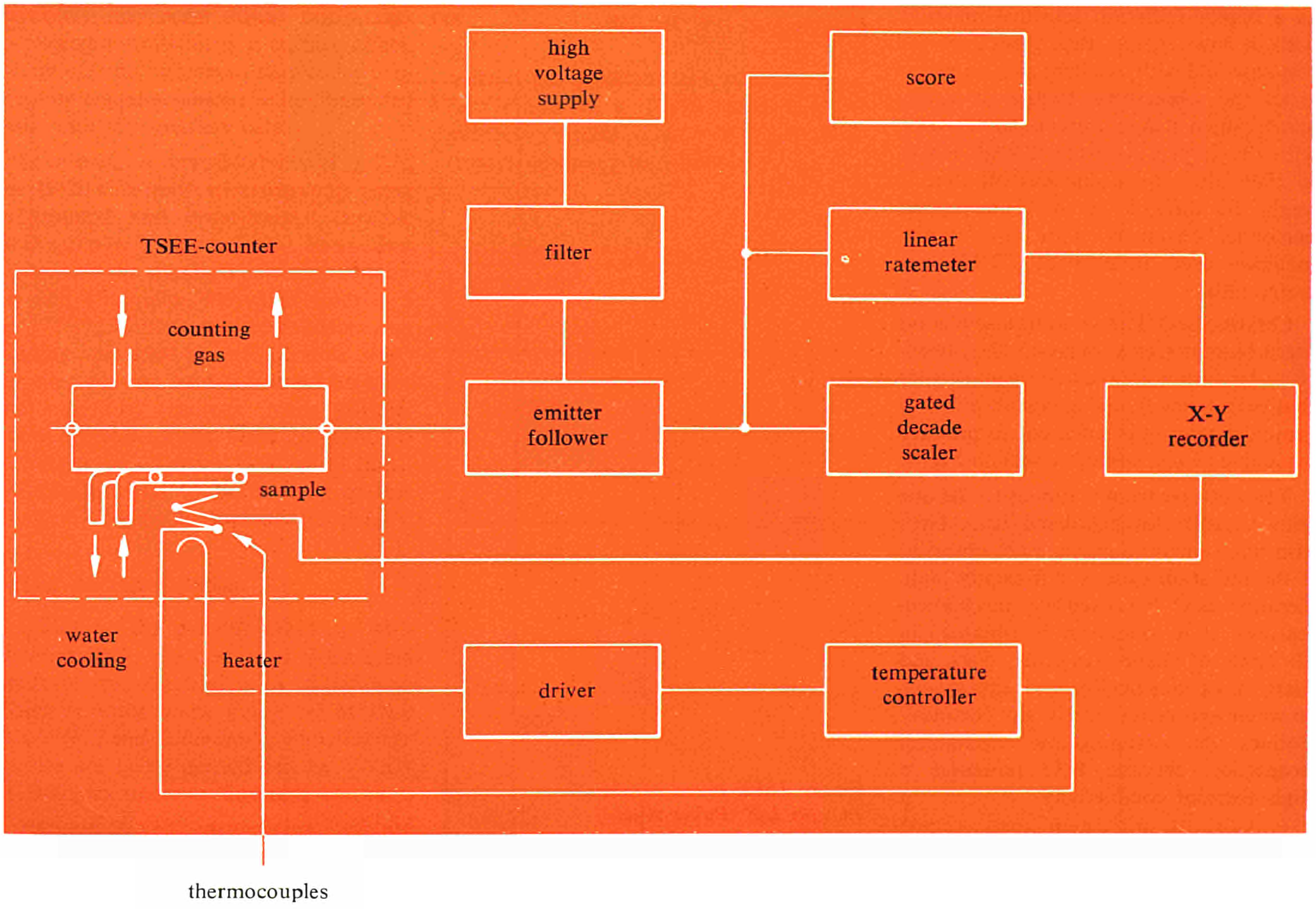

Fig. 4: *Block diagram of the accessory instrumentation for the counter. The pulses from the counter are fed into an emitter-follower preamplifier; from there they enter a gated decade scaler which is followed by a linear count-ratemeter. The output of the ratemeter is fed into the Y-input of an X-Y recorder, the X-input of which is connected to a thermocouple mounted on top of the heating element. The recorder thus registers the count-rate of the* TSEE *counter as a function of the sample temperature.*

---

[2] Linear Energy Transfer

radiator were used together with the *EE* material.

Some of the materials, such as LiF and BeO, are also very attractive because the photon energy dependence of the exoelectron emission is rather flat.

Further advantages of exoelectron dosimetry are the large variety of suitable substances. Besides the curves already mentioned, these include $CaF_2$, $BaF_2$, $SrF_2$, some sulphides, $Li_2B_4O_7$ and other metallic oxides apart from BeO.

The materials can be taken from the chemist's shelf, are inexpensive and need no complicated pretreatment (often annealing by the heating-cycle itself within the reader is sufficient). Sample preparation is also simple, no sophisticated technique is necessary for evaluation and the samples may be re-used if the reading does not require excessively high temperatures (deep trap depth).

Particular attention is at the moment being devoted to sintered ceramic BeO as a highly radiation sensitive material with a low energy dependence of its response and with excellent storage properties (no observable fading at room and elevated temperatures). *TSEE* work with this material started in Oak Ridge in 1969 after it became evident that it might be difficult to build a rugged personnel dosimeter with any of the materials used hitherto for *TSEE* dosimetry (20).

Ceramic BeO, known to be also a good thermoluminescence material (21), proved to be such a good exoelectron emitter that even a few hours' exposure to background radiation is sufficient to produce evaluable peaks, as can be seen in Fig. 9.

The trap spectrum is similar to the one shown earlier for powdered BeO. Here also three emission maxima are observed if the radiation dose is sufficiently high. Ceramic BeO has excellent mechanical features. It is solid, can be obtained in all kinds of shapes (as rods, discs and plates of various thickness), is impervious to water and resists nearly any chemical. Besides its advantageous mechanical properties, ceramic BeO possesses a high thermal conductivity.

Some drawbacks, which might possibly be overcome, help up the design of a personnel dosimeter with ceramic BeO.

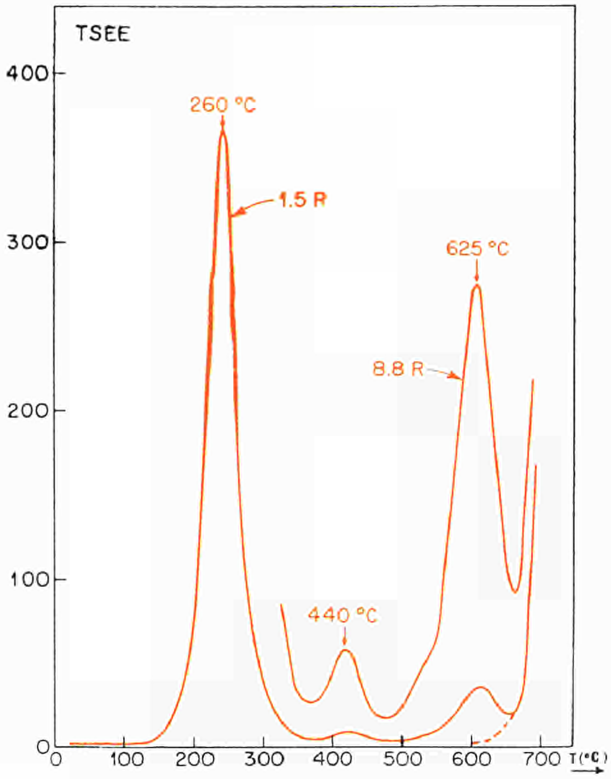

Fig. 5: *TSEE curve obtained with BeO (UOX, raw material from Brush Beryllium Co.) irradiated with gamma radiation. Heating rate: 1 °C/sec* (24).

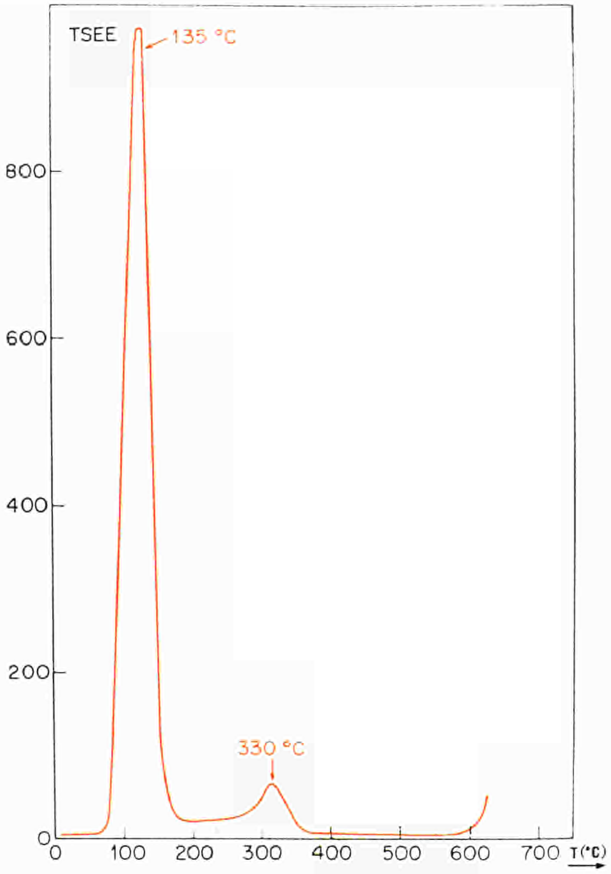

Fig. 6: TSEE *curve obtained with LiF (Baker Anal.), irradiated with 154 R Cs-137 gamma radiation. Heating rate 1 °C/sec.*

The first is that the ceramics used now exhibit a non-linear dose response. This is demonstrated in Fig. 10, which shows how the sensitivity, expressed in counts per R of gamma-radiation, decreases for increasing doses.

If the surface conductivity of the samples is increased, this sensitivity decrease with the dose is reduced (22), which is one way to overcome the drawback. Another problem at the moment is the energy dependence of the material, which has not hitherto been measured correctly. Also, calculation is difficult, as the exoelectron emission is a surface effect. Unless the radiation sensitive layer is covered by a sufficiently thick electron equilibrium layer, the surface layer will respond to electrons from surrounding materials like the air and supporting materials. More work is being done on this subject at present. A more serious problem—and this applies to the whole field of exoelectron dosimetry—is the poor reproducibility of the data. The reason for this is, again, that exoelectron emission is a surface effect. Many outside influences may cause exoelectron emission which can be eliminated only with the greatest care.

In one case a reproducibility of ± 2 % for 10-20 successive measurements using gold-plated and brass-framed ceramic BeO samples is reported (23). In another laboratory the standard deviation obtained with Thermalox 995 varies from ± 5 to ± 15 % for the repeated exposure and reading of gold-plated ceramic BeO samples with no heat treatment between the individual readings. Nude samples showed better results. Here the standard deviation varied from ± 7 to ± 13 %. More effort has to be devoted to this problem in order to obtain better results.

## Actual dosimeter design

Owing to the present problems with ceramic BeO, the design of dosimeters made of this material is in its infancy. There is some work going on at *Oak Ridge National Laboratory*, while further studies are being carried out by *CNEN* at Bologna under a Euratom contract.

Various *TSEE* dosimeters, mainly using BeO powder as the active layer, are described by Kramer (15). No commercial *EE* dosimeter is available yet; a first model of a *TSEE* reader with a gas-flow counter is on sale by an electronics company in Munich.

Fig. 7: *Optically stimulated exoelectron emission of* $SrSO_4$ *and BeO powder mixed with graphite, after irradiation with 10 keV X-rays* (18).

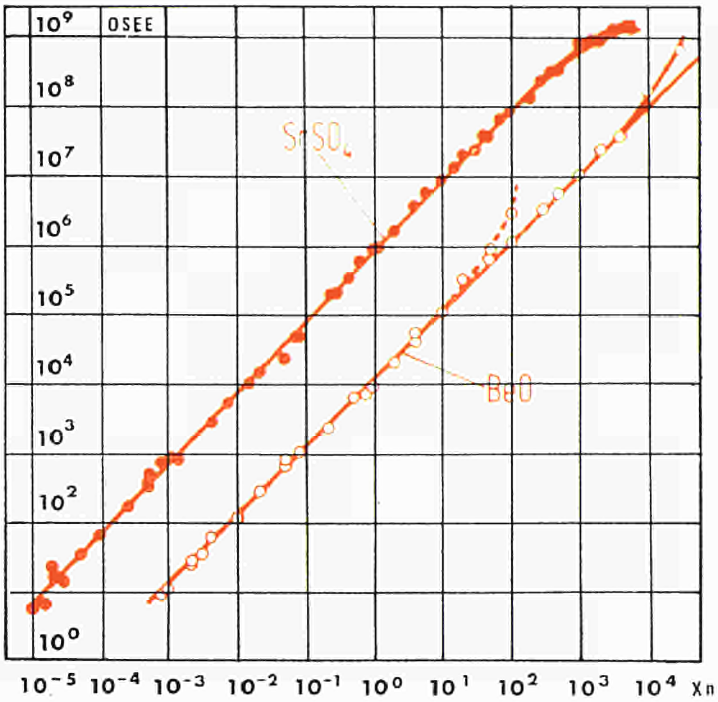

Fig. 8: TSEE *curves obtained with* $CaSO_4$ *(non-linear heating rate) after exposure to alpha particles and gamma radiation* (19).

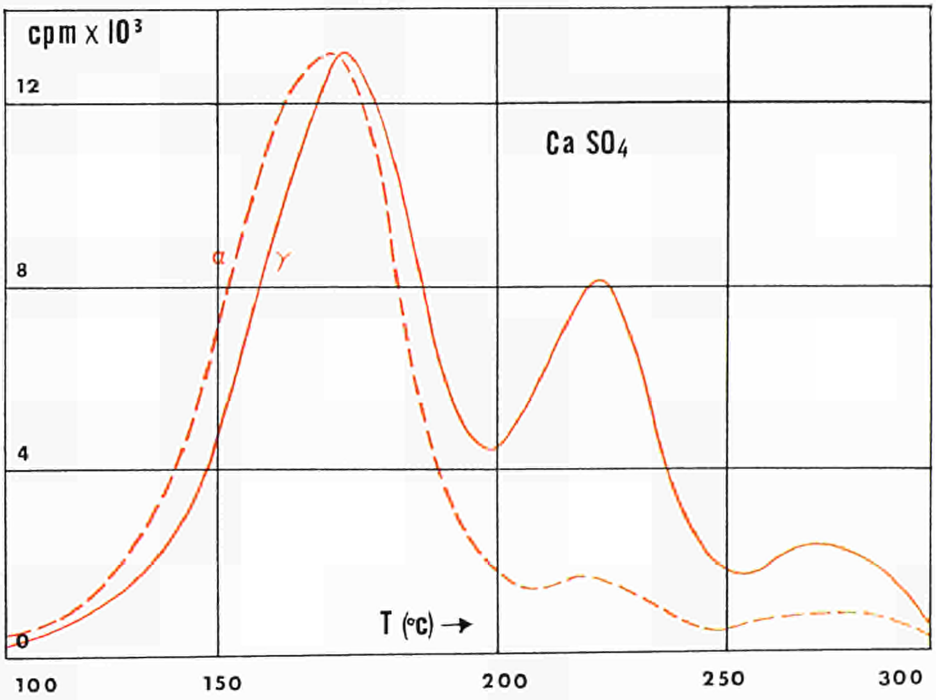

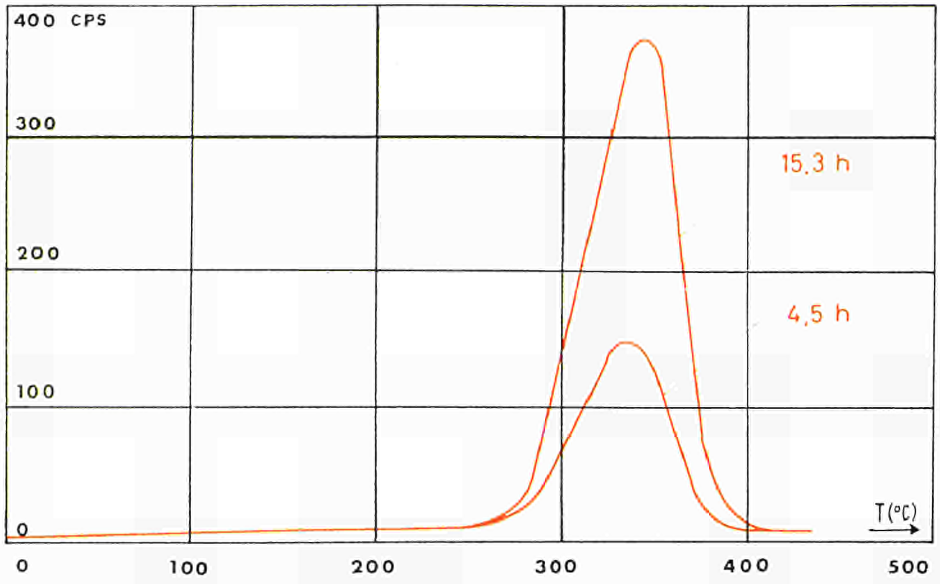

Fig. 9: *Background radiation* TSEE *curves (1 °C/sec) for ceramic BeO (Thermalox 995 background exposure). Storage time: 4.5 and 15.3.*

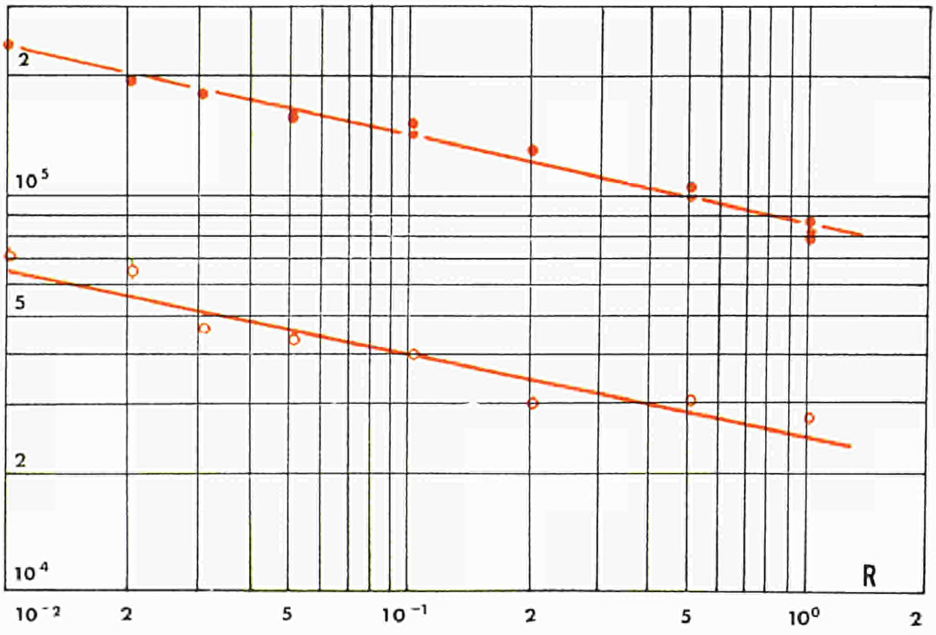

Fig. 10: *Gamma radiation sensitivity of ceramic BeO as a function of exposure. Upper line: counts/R obtained by evaluating first peak (175-375 °C);*

*Lower line: counts/R obtained by evaluating second and third peaks (375-600 °C).*

(23). *As can be seen, the sensitivity (expressed in counts per R of gamma radiation) decreases with increasing doses.*

### Further development of EE dosimetry

Certainly more effort will have to be made in order to improve the dosimetric characteristics of the ceramic BeO which might be contemplated for use not only in routine personnel dosimeters, but also as a highly sensitive dosimeter for gonad-dose measurements around X-ray installations, as a device for measuring background radiation (site survey, for example) and for special low-level radioactivity studies, such as the measurement of the distribution of gaseous effluents from reactor stacks or of the activity of low-energy particle-emitting radionuclides in liquids.

The very thin active layer of *EE* materials points to their suitability for measuring doses at interfaces (e.g. bone/tissue interfaces) and dose profiles of narrow beams and for certain micro-dosimetric problems.

The high upper dose limit of some materials might lead to new in-pile dosimeters, while the extreme sensitivity of others might produce very small dosimeters with a diameter of the order of some tenths of a micron.

Much attention will be paid to optical stimulation, which makes it possible to cover dose ranges with one reader which with thermal stimulation could be covered only by several measuring methods.

EUSPA 11-19

**Bibliography:** (1) J. ELSTER, H. GEITEL: *Ann. Phys.* (Leipzig), 59 (1896), p. 487. (2) J. KLAPHECKE: *Z. Phys.*, 67 (1931), p. 478. (3) J. KRAMER: Der metallische Zustand, Göttingen, *Vandenhoeck und Ruprecht* (1950). (4) J. KRAMER: *Z. Angew. Phys.*, 15 (1962), p. 20. (5) J. KRAMER: *Acta Phys. austriaca*, 10 (1957), p. 392. (6) J. KRAMER: *Z. Angew. Phys.*, 20 (1966), p. 411. (7) W. HANLE: *Acta Phys. austriaca*, 10 (1957), p. 339. (8) J. KRAMER: *Z. Phys.*, 133 (1952), p. 629. (9) J. KRAMER: *Naturw.*, 41 (1954), p. 160. (10) G. BARTHOW: *Naturw.*, 45 (1958), p. 381. (11) B. SUJAK: *Acta phys. polon.*, 20 (1961), p. 969. (12) A. R. KRASNAJA et al.: *Opt. Spektr.*, 12 (1962), p. 526. (13) G. HOLZAPFEL: *Phys. Stat. Sol.*, 33 (1969), p. 235. (14) W. HANLE, Z. SCHARMANN, G. SEIBERT, J. SEIBERT: *Nukleonik*, 8 (1966), p. 129. (15) J. KRAMER: Proc. Second Inter. Conf. on Luminescence Dosimetry - *USAEC Rep. Conf.* (1968), p. 180. (16) K. BECKER: Proc. Second Inter. Conf. on Luminescence Dosimetry - *USAES Rep. Conf.* (1968), p. 200. (17) W. KRIEGSEIS, A. SCHARMANN, J. SEIBERT: *Kerntechnik*, 13 (1971), No. 1, p. 11. (18) J. KRAMER: Proc. Third Inter Symp. on Exo-electrons, *PTB-Mitteilungen* 80, No. 5 (1970). (19) K. BECKER, N. CHANTANAKOM: *Nucl. Instr. a. Meth.*, 66 (1968), p. 353. (20) E.M. ROBINSON, M. OBERHOFER: *Health Phys.*, 18 (1970), No. 4, p. 434. (21) E. TOCHILIN, N. GOLDSTEIN, W. G. MILLER: *Health Phys.*, 16 (1969), p. 1. (22) J. F. WILSON: M. S. Thesis, Univ. Tennessee, *to be published.* (23) K. BECKER: Proc. Third Inter. Symp. on Exoelectrons, *PTB-Mitteilungen* 80, No. 5 (1970). (24) M. OBERHOFER, E. M. ROBINSON: *Kernt. Isotopent. u. Chemie*, 12 (1970), No. 1, p. 34.

# *Index 1972*

## authors

*Spec. = Special issue devoted to scientific information in the Community.

## subject

*Spec. = Special issue devoted to scientific information in the Community.

# *Index to Technical Notes 1972*

(left: serial number of notes; right: issue and page.)

# *First European congress on documentation systems and networks*

The Commission of the European Communities will hold a *First European Congress on Documentation Systems and Networks* from 16 to 18 May 1973 in Luxembourg.

There will be three sessions dealing respectively with:

- Input operations: data collection and storage;
- Processing methods – products and services;
- Financial and management aspects.

The working languages will be: English, French and German.

The congress will be preceded by a Seminar entitled "*the Anatomy of an Operational Documentation System*" which will be held on 14 and 15 May 1973.

Persons intending to submit papers should contact one of the three organizers before 15 November 1972:

- Institut français de Formation permanente (I.F.F.P.) 14, Rue Gramme, Paris (XV$^e$) (attn. Mrs. STERN – Tel. 727 75 09).
- Bureau Marcel van DIJK, 409, Avenue Louise, 1050 Bruxelles (Tel. 48 66 97).
- Commission of the European Communities, DG Dissemination of Information, 29, rue Aldringen, Luxembourg (attn. Mr. EMRINGER – Tel. 2 92 41, ext. 360).

# Just published

## Reports 1972

- **Deep penetration of neutrons in hydrogenous shields.** *EUR 4743 e.*
- **Collectrons, self-powered neutron flux detectors.** *EUR 4775 e.*
- **Mikrodosimetrische Untersuchungen zur Energieübertragung schneller Neutronen an weiches Gewebe.** *EUR 4787 d.*
- **Kalibrierung von Vakuummessgeräten.** *EUR 4797 d.*
- **Variable dead time neutron counter for tamper resistant measurements of spontaneous fission neutrons.** *EUR 4801 e.*
- **Zur Messung der gespeicherten Energie und spezifischen Wärme von Metallen und Legierungen mit einem Differential Scanning Kalorimeter.** *EUR 4802 d.*
- **Manufacturing specification for high temperature thermocouples for use in nuclear irradiation experiments.** *EUR 4807 e.*
- **Code TAFE — Analyse numérique de problèmes thermiques en présence de rayonnement et de conductivités variables avec la température.** *EUR 4809 f.*
- **Extraction du plutonium des combustibles eau lourde par le procédé Saltex.** *EUR 4812 f.*
- **Viscosity measurement of fuel suspension under irradiation by means of VISIR-2 measuring device.** *EUR 4817 e.*
- **Transient heat conduction through heat producing layers.** *EUR 4818 e.*
- **Trace level determination of oxygen in organic coolants and ultra-micro determination of oxygen in C-H-O organic compounds.** *EUR 4822 e.*
- **Etudes préliminaires sur le rôle du zooplancton dans la constitution et le transfert de la matière organique au sein de la chaîne alimentaire marine en Mer Ligure.** *EUR 4823 f.*
- **Etude par absorption différentielle dans l'infrarouge des lipides et des polymères irradiés.** *EUR 4828 f.*
- **Calculations for fission neutron and gamma multiplicity measurements.** *EUR 4829 e.*
- **Spectrometer using NaI(Tl)-Ge(Li) detectors in coincidence and anti-coincidence for (n,gamma) investigations.** *EUR 4831 e.*
- **La formation postgraduée des scientifiques dans la Communauté Européenne.** *EUR 4832 f.*
- **Four computer codes for dynamic process inventory determination application in safeguards.** *EUR 4833 e.*
- **A timecoder for neutron time-of-flight experiments.** *EUR 4835 e.*
- **Interactive graphic version of S/360 continuous system modeling program : user's and system manual.** *EUR 4836 e.*
- **COSTAX-BWR - A numerical programme for the axial dynamics of BWR nuclear reactors.** *EUR 4837 e.*
- **Hydrogen as an energy vector: new future prospects for applications of nuclear energy.** *EUR 4838 e.*
- **JN-METD2 - A Fortran—IV programme for solving neutron transport problems with isotropic scattering in multilayer slabs by the $j_N$ method.** *EUR 4839 e.*
- **Measurement of correlation properties of the bubble field in two-phase flow.** *EUR 4840 e.*
- **C.C.R. ISPRA - Caratteristiche del sito.** *EUR 4841 i.*
- **Filling alloys for fast breeder fuel element conditioning.** *EUR 4857 e.*
- **Radioaktive Kontamination von Lebensmitteln in den Gemeinschaftsländern im Jahre 1970.** *EUR 4858 d/f/i/n.*
- **Transient heat conduction through a cylindrical three-layer hollow fuel element with internal and external cooling.** *EUR 4862 e.*
- **Studies on the radioactive contamination of the sea.** *EUR 4865 e.*
- **Recommandations sur les mesures des irradiations reçues par les matériaux de structure de piles.** *EUR 4867 f.*
- **Application of atomic energy in agriculture.** *EUR 4868 e.*
- **Isolamento e determinazione di protoattinio-231 nelle urine.** *EUR 4870 i.*
- **A possible function for RNA to DNA inverted transcription in antibody biosynthesis and irreversible differentiation.** *EUR 4871 e.*
- **Survey of fusion reactors technology.** *EUR 4873 e.*
- **Un modello per la termoidrodinamica di un reattore ad acqua a canali « aperti ».** *EUR 4883 i.*
- **CAMAC - A modular instrumentation system for data handling.** *EUR 5100 e.*

These publications can be obtained at the *Sales office for official publications of the European Communities*, 37, rue Glesener, Luxembourg.

## ORDER FORM

I wish to subscribe to the **English/**.......... edition* of **euro-spectra** for one year at the price of :

Europe : 180 Belgian Francs
Other countries : 220 Belgian Francs

as from ....................................................

Name ....................................................

Full address ....................................................

....................................................

....................................................

....................................................
(Signature)

☐ Please invoice me.

☐ I am sending my remittance forthwith by money order/transfer/cheque to the order of A.M.P. (enclosed).

* Besides the English edition, **euro-spectra** is published in German, French, Italian and Dutch.

---

ORDER FORM

I wish to subscribe to the English/.......... edition* of euro-spectra for one year at the price of :

Europe : 180 Belgian Francs
Other countries : 220 Belgian Francs

as from ....................................................

Name ....................................................

Full address ....................................................

....................................................

....................................................

....................................................
(Signature)

☐ Please invoice me.

☐ I am sending my remittance forthwith by money order/transfer/cheque to the order of A.M.P. (enclosed).

* Besides the English edition, euro-spectra is published in German, French, Italian and Dutch.

---

ORDER FORM

I wish to subscribe to the English/.......... edition* of euro-spectra for one year at the price of :

Europe : 180 Belgian Francs
Other countries : 220 Belgian Francs

as from ....................................................

Name ....................................................

Full address ....................................................

....................................................

....................................................

....................................................
(Signature)

☐ Please invoice me.

☐ I am sending my remittance forthwith by money order/transfer/cheque to the order of A.M.P. (enclosed).

* Besides the English edition, euro-spectra is published in German, French, Italian and Dutch.

ca chemie chemistry biologie biologie biologia biologie biology medizin médecine medicina geneeskunde medicine werkstoffe matériaux materiali materialen materials ingenieurstechnik und geräte mécanique et appareillages ingeneria e attrezzature tecniche mechanika en apparatuur engineering and equipment kernreaktoren réacteurs nucléaires reattori nucleari nuclear reactors radioisotope radio-isotopes radioisotopi radioisotopen radioisotopes information und dokumentation information et documentation informazione e documentazione informatie en documentatie information science ozeanographie océanographie oceanografia oceanografie oceanography meteorologie météorologie meteorologia meteorologie meteorology Umweltbelästigungen nuisances inconvenienti ambientali milieuhygiene nuisances neue Verkehrsmittel moyens de transport nuovi mezzi di trasporto nieuwe vervoermiddelen new means of transport informatik informatique informatica informatieverwerking data processing fernmeldewesen communications comunicazioni communicatie communications physik physique fisica fysica physics chemie chimie chimica chemie chemistry biologie biologie biologia biologie biology medizin médecine medicina geneeskunde medicine werkstoffe matériaux materiali materialen materials ingenieurstechnik und geräte mécanique et appareillages ingeneria e attrezzature tecniche mechanika en apparatuur engineering and equipment kernreaktoren réacteurs nucléaires reattori nucleari nuclear reactors radioisotope radio-isotopes radioisotopi radioisotopen radioisotopes information und dokumentation information et documentation informazione e documentazione informatie en d

CDAA72004ENC